

3D Printing of Polymer Hydrogels—From Basic Techniques to Programmable Actuation

Fatih Puza and Karen Lienkamp*

This review discusses the currently available 3D printing approaches, design concepts, and materials that are used to obtain programmable hydrogel actuators. These polymer materials can undergo complex, predetermined types of motion and thereby imitate adaptive natural actuators with anisotropic, hierarchical substructures. 3D printing techniques allow replicating these complex shapes with immense design flexibility. While 3D printing of thermoplastic polymers has become a mainstream technique in rapid prototyping, additive manufacturing of softer polymers including polymer hydrogels is still challenging. To avoid deliquescence of printed hydrogel structures, the polymer inks used for hydrogel manufacture need to be sheer-thinning and thixotropic, with fast recovery rates of the high viscosity state. This is achieved by adding polymer or particle-based viscosity modifiers. Further stabilization of the interfaces of the printed voxels, e.g., by UV cross-linking, is often also required to obtain materials with useful mechanical properties. Here state-of-the-art techniques used to 3D print stimulus responsive, programmable polymer hydrogels, and hydrogel actuators, as well as ink formulation and post-printing strategies used to obtain materials with structural integrity are reviewed.

or sequential responses.^[1] This can only be achieved with a certain level of structural complexity. Such complexity is found in the natural materials formed by many organisms. These materials can adapt repeatedly and reliably to changes in the dynamic ecosystem that is the habitat of the organism, and thereby contribute to its survival and to advantages over non-adapting species.^[2]

In many natural tissues, built-in stimulus-responsive features, so called actuators, can trigger motion. These structures respond to changes in local mechanical stresses, light intensity, temperature, pressure, humidity, pH value, or the chemical composition of the environment. With different types of actuations (e.g., opening-closing cycles, bending, twisting, contraction or elongation), they directly modulate the properties of certain tissues. The actuators found in adaptive natural materials often consist of hierarchically organized, anisotropic topographies.^[3,4]

For instance, pinecone seed scales consist of a several millimeter thick bilayer of cellulose microfibrils with the orthogonal orientation of the fiber axes in each layer, and substructures on the micrometer length scale. These features enable a differential response to humidity changes by different degrees of swelling in each layer, which leads to bending.^[5,6] Similarly, the seed pod openings of various plants have bilayer structures that undergo anisotropic deformation with environmental humidity changes, which leads to opening and closing of the pods.^[7]

Research on adaptive soft materials and actuators that take their inspiration from nature has increased significantly in the past two decades. Some of the materials that were developed since then have reached such a high level of complexity in their structures, and intricacy in the tasks they perform, that it is not an exaggeration to call them “programmable.” For example, synthetic soft actuators that can convert relatively small external stimuli into large mechanical deformations were reported, so that the complex types of motion found in natural actuators could be emulated or even surpassed.^[8–10] Similarly to their natural archetype, these synthetic programmable materials have dynamic hierarchical structures that enable customized and on-demand response to a specific environment. This makes them attractive candidates for applications, for example in robotics^[11] and the biomedical sciences^[12] (in drug delivery,^[13] or the construction of artificial muscles^[14]). Different kinds of soft materials, such as dielectric elastomers, liquid crystalline elastomers, shape memory polymers, and hydrogels have already been used

1. Introduction

Scientists use the terms “stimulus-responsive” and “adaptive” when describing materials that undergo structural changes in consequence of an external stimulus. In contrast, the term “programmable” refers to materials that have been designed to change specific properties on-demand and in a precise, predetermined way, in analogy to a mechanical robot programmed to perform a task using software. Thus, in contrast to the more simple stimulus-responsive and adaptive materials, which can only perform one-way tasks such as irreversible deformation, programmable materials are able to show reversible, periodic,

F. Puza, K. Lienkamp
Professur für Polymerwerkstoffe
Fachrichtung Materialwissenschaft und Werkstoffkunde
Universität des Saarlandes, Campus
66123 Saarbrücken, Germany
E-mail: karen.lienkamp@uni-saarland.de

 The ORCID identification number(s) for the author(s) of this article can be found under <https://doi.org/10.1002/adfm.202205345>.

© 2022 The Authors. Advanced Functional Materials published by Wiley-VCH GmbH. This is an open access article under the terms of the Creative Commons Attribution-NonCommercial-NoDerivs License, which permits use and distribution in any medium, provided the original work is properly cited, the use is non-commercial and no modifications or adaptations are made.

DOI: 10.1002/adfm.202205345

in this context.^[15] In the following, we will focus on 3D printable programmable materials based on polymer hydrogels.

Hydrogels are a subgroup of polymer networks and consist of cross-linked hydrophilic polymers. Depending on the cross-linking density and the nature of their repeat units, they can bind large amounts of water.^[16] With a high water content and low elastic modulus, they are similar to the soft tissues found in the human body. Biocompatibility can be obtained if the chemical structure is properly balanced. Hydrogels swell and deswell when their environmental conditions (e.g., solvent quality, ionic strength, temperature, pH value) are changed, which can be used for actuation. Additionally, they can be scaffolds for active components, i.e., materials that are susceptible to external stimuli, such as particles with electric or magnetic properties, or redox activity.^[17–19] Thus, hydrogels provide a synthetic platform from which materials with multiple levels of stimulus-responsiveness can be constructed. Hydrogel actuators that are susceptible to light,^[20,21] temperature,^[22,23] magnetic fields,^[24] and ionic interactions^[25] have been reported. When exposed to these external stimuli, the hydrogel network structure undergoes a shape transformation and reorganization on the molecular scale, which leads to macroscopic actuation.^[16] Depending on the applied stimulus, this reorganization can be caused by direct changes in the swellability of the hydrogel scaffold, or is affected by the active components embedded into the network.

Hydrogels can be processed by various techniques to obtain objects with well-defined shapes and programmable actuation. Many types of hydrogel actuators that have been developed so far were fabricated by molding,^[26] soft lithography,^[27] or photolithography.^[28] These kinds of fabrication methods have various limitations. They either require expensive molds or lithographic masks, are multistep processes, or may be unsuitable to produce objects with complex geometries. For example, photolithography is a multistep process that requires a lithographic mask that gets increasingly more expensive the finer the structures to be reproduced are. Also, the actuator layers obtained by this technique are only 2D, relatively thin and often not self-standing. Sequential layer deposition of these layers to assemble 3D actuators is possible but requires precise alignment of each consecutive layer, as well as further processing steps for layer bonding.^[28] Due to the limitations and complexity of the above-mentioned traditional technologies, 3D printing has become a promising alternative for the manufacture of polymer hydrogels. Thanks to technological advances in the past years, 3D printers have become widespread and increasingly more affordable. They enable rapid, low-cost manufacturing of objects with on-demand geometries and relatively high structural resolution (significantly below 100 μm for high-end machines).^[29,30] The design of printing files for self-standing complex structures, the so-called “slicing,” is assisted by various software packages,^[31] making the technique accessible to the general and scientific public. What makes 3D printing unique for the manufacture of actuators and programmable materials is the possibility to precisely control the properties of each printed volume element (“voxel”), which generates unprecedented levels of design freedom. Printing parameters like the layer and voxel dimensions, the print pattern and orientation, as well as the voxel composition, can be easily controlled during the material deposition, so that the desired properties of the target material can be precisely adjusted. Thus, 3D printed hydrogels with com-

plex structures that can mimic the actuation modes of natural stimulus-responsive materials are accessible.^[32] In particular, the structural anisotropy found in natural tissues can be easily emulated in 3D printed hydrogels. Also, the 3D printing process itself gives access to another level of structural anisotropy: at a sufficiently high ink viscosity, the shear forces applied during printing can stretch the polymer chains into nonequilibrium conformations (which can be locked in by UV cross-linking), and elongated additives such as micro- and nanoscale rods can be aligned parallel to the printing direction. These features can be used to enable actuation.^[33]

This review discusses the currently available 3D printing approaches, design concepts, and materials that are used to obtain programmable hydrogel actuators. First, the fundamentals of 3D printing and the special conditions needed to print hydrogels will be introduced. Following that, programmable hydrogel actuators with different types of stimulus responsiveness will be presented, together with an outlook on the open challenges for the field.

2. Engineering Aspects: 3D Printing Technologies for Polymer Hydrogels, and Hydrogel Actuator Design Concepts

2.1. Programming Soft Matter Actuation with 3D Printing

Using 3D printing, hydrogel materials and their precursors can be shaped into objects that can be actuated on demand and with fairly high spatial resolution (**Figure 1**). Thus, sophisticated hydrogel designs can be realized, and complex programmed actuation modes are accessible. Two strategies are mainly used for this purpose: so-called “bulk material programming,” where the hydrogel is programmed by incorporating compositional changes along its macroscopic dimensions, or “patterning,” where the hydrogel is printed from chemically uniform layers with grid-like patterns of varying sizes, shapes, and orientations. In bulk material programming, either gradients of the cross-linking density and/or the chemical composition are introduced,^[34] or an anisotropic distribution of the components is obtained, e.g., by shear-induced alignment during printing.^[35] When using patterning strategies, grids with different mesh sizes, shapes, orientation, and ratios of filled and open voxels are printed on top of each other. The actuation response of the materials thus obtained can be programmed by varying the orientation or angle of the grid,^[36] the grid type,^[37] or its surface area, along the z-axis of the material.^[38]

Figure 1a shows an example of the bulk programming approach. In this example, the 3D printed, bulk-programmed hydrogel material mimics a biological system with gradients in its mechanical properties due to compositional gradients. In natural soft tissues, these are obtained by self-assembly processes. Such gradients induce nonequilibrium conditions inside the material, e.g., an uneven distribution of internal stresses, which can be used for actuation. Obtaining such gradients in synthetic polymer materials with conventional techniques, e.g., in situ polymerization, is far from trivial. With 3D printing, gradients are accessible by adjusting the ink composition voxel by voxel. In each voxel, the monomer type and concentration, the

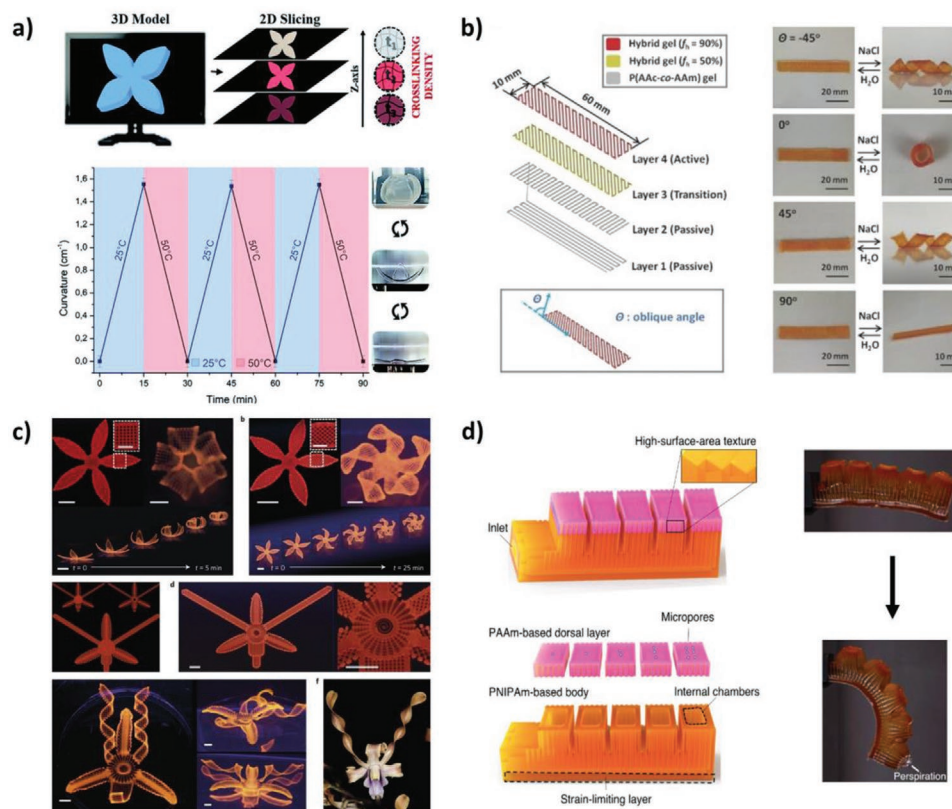


Figure 1. Examples of 3D printed programmable hydrogel actuators: a) Hydrogel printed from thermosensitive poly(*N*-isopropylacrylamide) (PNIPAm) with cross-linking density gradient in *Z*-direction. Due to different cross-linking ratios in each 2D slice, temperature changes induce different local macroscopic extension/contraction of the material. Reproduced with permission.^[34] Copyright 2019, The Royal Society of Chemistry. b) 3D printed hydrogel made from poly(acrylic acid-*co*-acrylamide) (P(AAc-*co*-AAM)) and poly(acrylic acid-*co*-*N*-isopropyl acrylamide) (P(AAc-*co*-NIPAm)) with a grid-like substructure. Variations in the substructure pattern angle led to different types of motion when actuation was triggered with concentrated saline solution. Reproduced with permission.^[36] Copyright 2018, Wiley-VCH. c) Hydrogel printed from different components (nanofibrillated cellulose with PNIPAm or *N,N*-dimethylacrylamide); each layer was printed using a different grid substructure. When the material was actuated by temperature changes, materials with different grid combinations had different bending characteristics. Reproduced with permission.^[37] Copyright 2016, Springer Nature Ltd. d) Actuation by combination of thermoresponsive materials and hydraulic forces: 3D hydrogels obtained by stereolithography consisting of a poly(acrylamide) (PAAm) dorsal layer with micropores, and a PNIPAm body with internal chambers. Above its LCST, the PNIPAm network collapses and reduces the volume of the chambers, so that water is pushed out of through the PAAm pores. The 3D printed pores control the water flow. Upon cooling, the opposite motion was obtained. Reproduced with permission.^[38] Copyright 2021, Springer Nature Ltd.

type and amount of additives for mechanical reinforcement, and the cross-linker density can be varied.^[39] In the example shown (Figure 1a), researchers printed flower-shaped poly(*N*-isopropylacrylamide) (PNIPAm)-based hydrogels which had a gradient of the comonomer 2-carboxyethylacrylate (CEA) and the cross-linker *N,N'*-methylenebisacrylamide (MBA) along the *z*-axis.^[34] This enabled folding of the flower leaves when the temperature was increased above the lower critical solution temperature (LCST) of PNIPAm. Another recently reported 3D printed hydrogel had gradients in Ca^{2+} and Fe^{3+} ion concentration, which affected the local gelation of its alginate matrix loaded with magnetic nanoparticles.^[40] Thus, the local elastic moduli of the hydrogels could be adjusted, so that an anisotropic actuation in response to an external magnetic field was obtained.^[40]

Figure 1b illustrates the patterning approach. 3D printed hydrogels consisting of patterned layers can be used to imitate such structural hierarchy often found in living tissues. In these biomimetic materials, patterns with different grid types,

dimensions, or orientation are used to obtain anisotropic actuation in response to external stimuli. Figure 1b shows a 3D printed hydrogel consisting of layers of poly(acrylic acid-*co*-acrylamide) (P(AAc-*co*-AAM)) and poly(acrylic acid-*co*-*N*-isopropyl acrylamide) (P(AAc-*co*-NIPAm)) with different grid orientation.^[36] Variations of the angle of the top layer relative to the lower layers led to different types of motion (twisting, rolling) due to anisotropic swelling when the material was immersed into a concentrated saline solution.^[36] Similar hydrogels with different grid orientation were printed from PNIPAm or *N,N*-dimethylacrylamide that additionally contained cellulose nanofibers. When the materials were actuated by temperature changes, they folded or twisted into different directions (Figure 1c).^[37] Internal structuring of 3D printed hydrogels on larger dimensions has also been reported. As shown in Figure 1d, in one study stereolithography was used to print a structure with internal chambers from thermoresponsive PNIPAm as the main body material, and poly(acrylamide) (PAAm) with a micropore structure as the

chamber lids.^[38] When temperature was increased above the LCST of PNIPAm (40 °C), that hydrogel part collapsed, so that the size of the chambers decreased. The encapsulated water built up sufficient internal pressure to be pressed through the PAAm micropores. When cooling down, the PNIPAm layer returned to its original geometry.

These examples illustrate the degree of flexibility provided by 3D printing when designing programmable biomimetic actuators. Depending on the desired actuation features, different types of 3D printing methods and materials can be chosen from. In the following subsections, we will look more closely at the 3D printing methods used to obtain programmable hydrogels.

2.2. 3D Printing Technologies for Soft Matter, Including Polymer Hydrogels

In the past years, different 3D printing techniques have been developed for diverse kinds of materials, including metals, polymers, ceramics, and other inorganic materials. It is even possible to print entire buildings from concrete with large-scale printing systems.^[41] This has been extensively reviewed before.^[42,43] In the field of polymers, 3D printing has evolved from melt-extrusion of thermoplastic filaments towards technologies that can handle liquid inks for polymer hydrogels, which are UV cross-linked in situ during the printing process or self-crosslink thermally. Depending on the printing method and the type of material used, the printing resolution of commercial instruments ranges from the tens of nm to the mm scale.

Overall, 3D printing technology used for soft matter can be classified as follows: i) extrusion printing, where continuous filaments are used as building blocks; ii) inkjet printing using low viscosity inks, often combined with in situ or post-fabrication processing to obtain mechanically stable structures; iii) stereolithography printing using photopolymerizable prepolymer solutions; iv) laser-assisted printing methods, where laser beams are used to construct complex structures from ink droplets. All these 3D printing methods require different ranges of material viscosities for the successful construction of 3D structured hydrogels, as summarized in **Table 1**. In the following sections, the different techniques are shortly explained, and their suitability for the production of hydrogel actuators is illustrated with examples.

Table 1. 3D printing methods used for soft matter: technology type, materials used, and process specifications.

3D printing technology	Material used for printing	Resolution in x,y direction	Viscosity of material
Extrusion printing	Filament or liquid ink	>100 μm ^[44,45]	6–30 × 10 ⁷ mPa s ^[46]
Inkjet printing	Liquid ink	50–500 μm ^[30]	3.5–12 mPa s ^[47]
Stereolithography	Polymer solution	<20 μm ^[48]	No limitation ^[49]
Laser-assisted printing	Liquid ink or polymer solution	10–100 μm ^[50]	1–300 mPa s ^[46]

2.2.1. Extrusion 3D Printing

In extrusion 3D printing, a polymer melt (obtained from a thermoplastic filament) or a viscoelastic polymer solution is pushed through a nozzle onto a substrate (the so-called print bed). Thus, a continuous flow of extruded material is obtained, which solidifies during cooling (in the case of molten thermoplasts) or during postprinting treatment such as UV irradiation (in the case of viscoelastic polymer inks). By moving the printhead holding the viscoelastic material along the printbed in the *x* and *y* direction, small objects can be built up voxel by voxel with a resolution of >100 μm, and a repeatability (i.e., the ability of the instrument to produce an identical object) on the same order of magnitude.^[51] Thus, extrusion 3D printing allows the processing of viscoelastic materials at precise processing temperatures and can be combined with optional post-printing treatment/curing steps such as UV exposure, heating, or solvent treatment to obtain smoother object surfaces. Extrusion printed materials generally have a high shape fidelity after deposition and post-treatment and yield comparatively large structures compared to other laboratory-scale 3D printing techniques.^[52] Typical extrusion 3D printers have printheads with nozzles that are 100 μm to 1 mm in diameter. The nozzle size can be used to control the dimensions of the deposited molten filaments or inks, and thus the voxel size. Depending on the nozzle size and geometry, fibers and other anisotropic components of the extruded material are aligned in flow direction, or remain randomly distributed.^[53] Printheads can be driven mechanically or pneumatically. Pneumatic setups use compressed air for extrusion, which works well for moderate viscosities, while mechanical systems with a piston or screw are needed to print highly viscous materials. As the printbed is the place where solidification or gelation of the printed product occurs, it is often equipped with heating or cooling devices, and sometimes also with light sources for UV cross-linking. Commercially available 3D printing filaments are mostly thermoplastic materials which become viscoelastic at elevated temperatures. They solidify after extrusion printing without further treatment. Inks used to print polymer hydrogels are viscoelastic under ambient conditions and need post-treatment by heating or UV irradiation to stabilize their final shape. For successful extrusion 3D printing, the hydrogel precursor inks or melts need a viscosity in the range of 6 to 30 × 10⁷ mPa s, which is higher than for other 3D printing techniques. They also should be shear-thinning. If these parameters are well-met, a continuous flow through the nozzle is achieved, and long fibers can be formed. Shear-thinning inks contain large chemical entities (e.g., macromolecules or particle-based rheology modifiers) whose intermolecular interactions can be easily broken when shear forces are applied. They can also be aligned in the direction of the shear-induced flow.^[54] The viscosity of inks used for printable hydrogels found in the literature covers a broad range, as the viscoelastic behavior of each system is impacted by the intrinsic properties of the applied polymer and rheology modifier. Additionally, the optimum viscosity for each system is affected by the printing hardware and the operating conditions. For this reason, the most useful viscosity values and the ideal shear-thinning behavior of each ink have to be determined experimentally for each specific 3D printing system (consisting

of the ink, the printer, and the operating parameters). At the optimum viscosity, inks are able to flow continuously without disruption of the printed viscoelastic filament. The upper viscosity limit is determined by the need to avoid clogging of the printer. Also, a too high ink viscosity leads to noncontinuous filament flow and to defective printed structures. In contrast, a too low ink viscosity leads to deliquescence of the printed structure and a lower printing resolution.^[55] With reference to shear thinning, it is advisable to tune the system parameters such that the ink viscosity decreases at least one order of magnitude during printing, and has a fast recovery of the high viscosity state. For example, 3D printable PEG/laponite hydrogels decrease in viscosity from $\approx 10^4$ to ≈ 1 Pa s when the shear rate is swepted from 10^{-1} to 10^3 s⁻¹.^[56] It goes without saying that the ink viscosity value also significantly affects the physical properties of the printed structures.^[46]

Inks with optimal viscosity for printing can be formulated by adjusting the type, molecular weight, and concentration of the polymer component used, and by adding rheology modifiers. The effect of these parameters is typically studied and optimized prior to printing by rheological measurements. In summary, due to the design flexibility provided, the large viscosity range of the materials that can be processed, and the possibility to make relatively large structures compared to other 3D printing techniques, extrusion 3D printing is the most promising technique for the design and production of programmable hydrogel actuators on the market (so far). It can be used both for the bulk material programming approach and the patterning approach described in Section 2.1, and the high viscosities of the inks used enable anisotropic alignment of ink and melt components during printing.

These features are illustrated by the extrusion 3D printed hydrogel actuators discussed below (**Figure 2**). In the example shown in Figure 2a, the shear forces present during extrusion 3D printing induced unidirectional alignment of cotton fibrils contained in the *N,N*-dimethylacrylamide-based ink formulation.^[37] In an aqueous environment, this 3D printed material would bend due to anisotropic swelling, while the distribution of the fibrils in solvent-cast hydrogels remained uniform, and the material did not show such actuation (Figure 2a).^[37]

In another study, a hydrogel was extrusion 3D printed from an ink consisting of laponite nanoclay, PNIPAm, and alginate (Figure 2b).^[35] Alignment of the nanoclay was observed during printing, as well as compositional changes that occurred when the shear forces were varied. Notably, in the examples shown, the alignment of the anisotropic components of the inks is not lost after removal of the shear force due to the rheological properties of the inks. While the shear-thinning properties of the ink combined with the processing shear enable the alignment, a fast recovery of the high viscosity state slows down diffusion processes that would otherwise destroy the thus obtained anisotropy. On the molecular level, the induced and persisting alignment is a consequence of the strong intermolecular interactions between the ink matrix material and the nanoclay platelets, by which the shear alignment of the polymer matrix is transmitted to the nanoclay.^[35] As a result of the anisotropic alignment of the filler, the material presented in Figure 2b would reversibly roll and unfold at different temperatures.

Depending on the cross-linker type used, the material would either roll above its LCST, or below.^[35] Using the patterning approach described in Section 2.1, Arslan et al. produced extrusion 3D printed hydrogels that contained continuously printed polyethylene glycol (PEG) fibers in a PNIPAm matrix, with different relative orientation of the PEG fibers in adjacent layers (e.g., 0°, 22.5°, and 45°) (Figure 2c).^[32] In order to mimic specific biological systems, different types of actuation were programmed into the material by adjusting these relative orientations. Thus, arc shapes ($\theta = 0^\circ$, pine cone-like), a cylindrical helix ($\theta = 22.5^\circ$, mimicking the coiled tendrils of climbing plants), and a helical twist ($\theta = 45^\circ$, as found chiral seed pods) could be obtained. These examples highlight the potential of extrusion 3D printing for further progress in designing programmable polymer hydrogels. While first principles have been explored, it has yet to be demonstrated that these interesting systems can be put to use outside the laboratory.

2.2.2. Inkjet 3D Printing

While the high shear forces exerted on inks and molten filaments during extrusion 3D printing can be used to align anisotropic ink components, they can be problematic for more sensitive ink elements, including biological components. Particularly if living cells are part of the ink, a lower viscosity is preferred, as cells and many biomolecules are susceptible to damage by high shear forces.^[57] Inkjet 3D printing was developed as a technology platform that would allow constructing 3D structures from low viscosity inks. Unlike extrusion 3D printing, where fibrous filaments are deposited, the inks used for inkjet 3D printing are deposited as small volume droplets. To achieve this, thermal or piezoelectric modules in the print-head split up the bulk ink (which has a typical viscosity from 3.5 to 12 mPa s) into droplets with a picoliter volume.^[47] The resolution of the structures printed from these inks is between 50 to 500 μm .^[30] While inkjet 3D printing is useful to build up thin structures on solid substrates, e.g. to print hydrogel-embedded cells onto a cell culture dish, or to print electronic circuits onto a chip, the technique has limitations to when it comes to fabricating self-standing structures. Due to their low viscosity, the ink droplets spread out, which not only limits the resolution in *x* and *y* direction, but also the height in *z* direction. Spreading of the printed droplets of the first layers of a structure can be restricted by hydrophobic modification of the substrate, which make surface wetting energetically unfavorable.^[58] For successful inkjet printing, good droplet coalescence is required, which also depends on the surface energy of the system.^[59]

As the method requires low viscosity inks, they contain only low mass fractions of polymer, which typically also have a lower molar mass. This results in lower elastic moduli and mechanical stability of the printed structures.^[60,61] Yet this can be remedied to a certain extent by postprinting treatment, i.e., ink-jetted objects that are built up layer-by-layer can be cured after each layer, either by thermally drying the ink, or by cross-linking it with UV light. In the field of hydrogel actuators, inkjet 3D printing has been used to build and anisotropically modify sodium alginate hydrogels. First, liquid sodium alginate polymer droplets were deposited on a

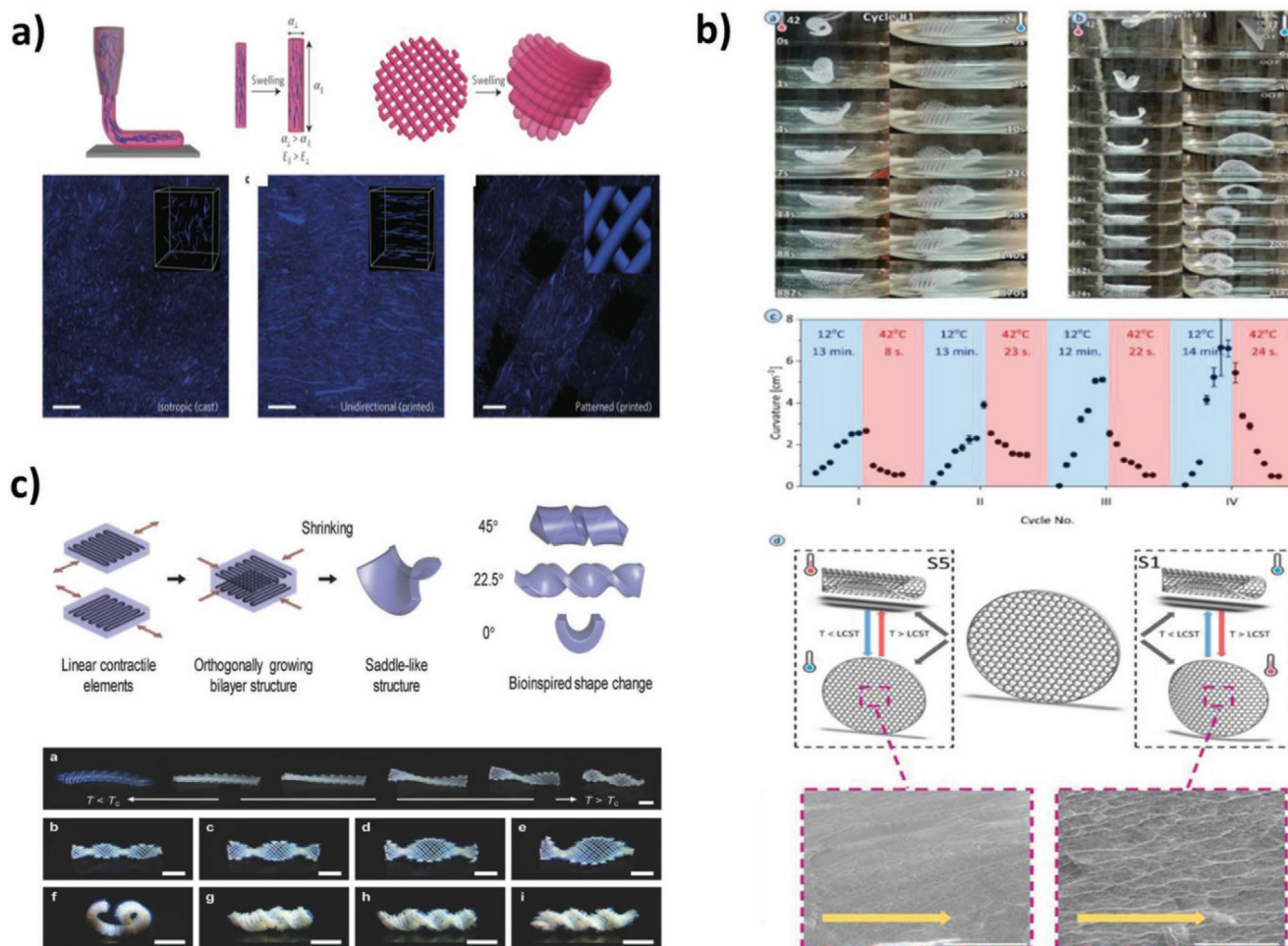


Figure 2. Hydrogel actuators fabricated by extrusion 3D printing: a) Shear-induced anisotropic alignment of cellulose fibrils in poly(*N,N*-dimethylacrylamide) hydrogels, leading to anisotropic swelling. During water uptake, these hydrogels start to bend. Reproduced with permission.^[37] Copyright 2016, Springer Nature Ltd. b) Extrusion 3D printed PNIPAM-alginate hydrogels with nanoclay fillers and different kinds of cross-linkers. Material S1 contained only one type of cross-linker, and rolls into a tube at $T < LCST$; material S5 with an additional cross-linker forms a tube at $T > LCST$. By going through several heating-cooling cycles, it could be shown that the effect was reversible. During 3D printing, the nanoclays were aligned anisotropically, as shown in SEM insets. Reproduced with permission.^[35] Copyright 2021, Wiley-VCH. c) Extrusion 3D printing of polyethylene glycol (PEG) filaments into thermoresponsive PNIPAM hydrogel networks. The presence and orientation of the filaments affect the local swelling of the hydrogels during the LCST transition, and thus cause the material to bend into different shapes, depending on the filament pattern used. Reproduced with permission.^[32] Copyright 2019, Wiley-VCH.

substrate. Following that, they were crosslinked by printing Ca^{2+} containing droplets onto the polymer droplets.^[62] Even if ink droplet coalescence is optimized, the mechanical properties of inkjet 3D printed hydrogels are inferior to those obtained by solvent casting. For example, inkjet printed sodium alginate hydrogels had an elastic modulus E of 56 kPa, with a strain at failure $\epsilon_{failure}$ of 112%, while the cast hydrogels that had the same mass fraction of polymer, and had undergone the same post-treatment, had an E of 95 kPa and an $\epsilon_{failure}$ of 158%.^[63] This difference is related both to defects from printing (like incomplete droplet coalescence), and to less molecular entanglements at the (former) droplet interfaces in the printed structures.

Inkjet 3D printing with reactive droplets is also useful in the context of hydrogel actuators to anisotropically pattern isotropic hydrogel substrates that were obtained by other methods, e.g., by

casting or molding. In this case, the ink is printed onto a hydrogel substrate and diffuses into it, thereby creating domains with higher elastic moduli than those of the unreacted surroundings.

Additionally, the chemical composition of the printed droplets can be tuned individually, or they can be applied in different patterns so that a locally differentiated responsiveness of the hydrogel is created.^[64] For example, a patterned programmable hydrogel system was developed by Peng et al. using droplets containing Fe^{3+} ions, which were deposited onto a poly(acrylate) hydrogel layer (Figure 3a).^[64] By complexation of the acrylate groups with the Fe^{3+} ions, the cross-linking density of the hydrogel was increased locally. When the thus patterned hydrogel was immersed into water, the swelling ratio in the exposed areas was lower than in the untreated areas, so that different actuation modes (flower-like bending, twisting, and/or rolling, Figure 3b) were observed.

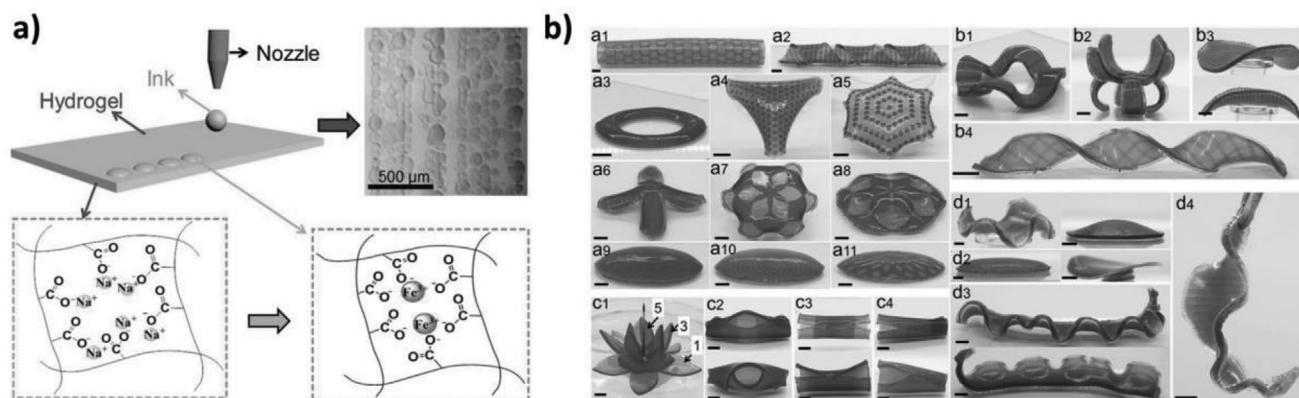


Figure 3. $\text{Fe}(\text{NO}_3)_3$ -containing droplets were inkjet 3D printed onto poly(sodium acrylate)-based hydrogels. The deposited ions locally cross-linked the acrylate groups. This anisotropy in the cross-linking density of the material changed its local swellability, leading to different modes of actuation in aqueous media. Reproduced with permission.^[64] Copyright 2017, Wiley-VCH.

Zhang et al. reported a similar inkjet 3D printing-based actuation strategy by depositing sodium hydroxide (NaOH) droplets onto PAAm hydrogels.^[65] The concentrated NaOH solution hydrolyzed the PAAm amide groups to negatively charged acrylate groups. The chemical anisotropy thus induced also altered the local swellability of the material. As the OH^- ions diffused through the material, the extent of amide hydrolysis varied along the thickness of the material, leading to a swellability gradient. The resulting hydrogel could be reversibly actuated into complex shapes and types of motion (e.g., tubes and helices, lotus leave-like closing) by changing the pH value and other solution parameters.^[65]

2.2.3. Stereolithography 3D Printing

The main limitations of the above-described 3D printing techniques are their structural resolution, and the need for a certain range of physical properties of the inks, which puts a number of constraints on the ink composition. Some of these shortcomings, in particular the resolution issue, can be overcome using stereolithography-based printing systems. For these, the theoretical resolution limitation is given by the wavelength of the light source, i.e., the UV light source. In practice, the resolution limit is in the range of a few micrometers. The inks used for this printing process contain photosensitive monomers that can be photopolymerized with this relatively high local resolution. A typical stereolithography 3D printer consists of a container for the monomer, a printbed mounted on a movable stage inside the container, and several movable micromirrors to control the path of the light beam used.^[66] Objects obtained by stereolithography 3D printing are polymerized layer-by-layer, while the printbed is moved in the z-direction, so that complex geometries are accessible.^[67] The wavelength and intensity of the light source and the exposure time are key factors that affect the resolution of the obtained structures. One advantage of using such an optical set-up, compared to the mechanically controlled 3D printing techniques discussed previously, is that it is possible to control the degree of cross-linking of each layer through the irradiation conditions,^[67] and that the viscosity of the ink is not limited by the printing process. In this respect,

it is fundamentally different from the previous technologies, where the range of usable inks was limited to inks with suitable rheological properties, and the resolution was restricted by the dimensions of the nozzle.^[68] Mishra et al. demonstrated that even PNIPAm inks with a viscosity of less than 10 Pa s, which is more than a factor of 100 less than the inks required for extrusion and inkjet 3D printing, could be successfully processed by stereolithography 3D printing.^[69] On the chemical side, the limiting factor for stereolithography-based 3D printing is that it requires photosensitive monomers that undergo sufficiently rapid photopolymerization. Acrylate-based monomers are very suitable for this purpose due to their high polymerization rates so that the construction of well-defined, high-resolution objects is possible.^[70] Another limitation of the method is that it is not possible to vary the resin composition from layer to layer, or voxel to voxel, as in the extrusion/inject 3D printing techniques.

The degree of cross-linking obtained during stereolithography 3D printing affects the mechanical properties of the resulting structures. Thus, it is clear that the efficiency of the photoinitiators used will strongly affect these properties. In the context of printing hydrogels by stereolithography, it is important to remember that the preferred medium to obtain hydrogels is aqueous solutions. Unfortunately, many photoinitiators are only poorly water soluble and therefore cannot be well dispersed in the reaction medium, yielding inhomogeneous polymer networks and materials with low elastic moduli.

Further homogenization (e.g., agitation or mixing with organic solvents) is needed to improve their solubility and distribute them homogeneously in the precursor monomer solutions.^[71] On the other hand, a limited number of water-soluble photoinitiators (e.g., 2-hydroxy-1-[4-(2-hydroxyethoxy)phenyl]-2-methyl-1-propanone, Irgacure 2959) are commercially available. However, their solubility is still not superb, and they are not functioning in an efficient way at wavelengths above 385 nm.^[72] For these reasons, new types of photoinitiators are needed for stereolithography-based hydrogel printing. For example, Pawar et al. developed a photoinitiator system based on 2,4,6-trimethylbenzoyl-diphenylphosphine oxide (TPO) nanoparticles, which are highly water dispersible, allowing homogeneous polymerization. This photoinitiator system can also efficiently work in a broad range of wavelengths (between 385 to

420 nm).^[71] When compared to commercial Irgacure 2959, the use of TPO photoinitiator nanoparticles enable easier printing and faster gelation as the nanoparticles trigger fast formation and distribution of free radicals among the monomer precursor. In case of hydrogel actuators, the poor water solubility of photoinitiators and wavelength limitations could lead to problems in the actuator's performance. Yet even if the composition of the precursor solution is the same during 3D printing, the degree of cross-linking of the hydrogel may change from layer to layer as the energy density of the light source depends on the length it travels through the reaction medium (due to Lambert-Beer's law). This either has to be compensated for by adjusting the energy density, or by choosing a reaction medium with negligible absorbance at the wavelength used for polymerization.

Still, due to its higher structural resolution, stereolithography 3D printing is an ideal choice for the fabrication of very small programmable hydrogel actuators. For example, Odent et al. used this method to print programmable multilayer hydrogels that had gradients in cross-linking density and surface patterning (Figure 1a). The gradients in cross-linking densities (from 0.6 to 1.8 mol cm⁻³) were obtained by varying the UV exposure times between 2 and 4 s. The resulting local differences in the stiffness and swellability of the 3D printed material led to locally different bending actuation in aqueous media.^[34] In another study, Ji et al. used stereolithography 3D printing to write microstructures on top of isotropic hydrogels and thereby induced anisotropic swelling of the material (Figure 4a).^[73] The

different orientations of the microstructures relative to the hydrogel axis led to diverse actuation modes during swelling. For example, perpendicular orientation of the structures caused bending of the hydrogel, while a 45° angle caused twisting. The actuation mode also depended on the UV exposure time during 3D printing, as this affected the degree of cross-linking (and thereby the swellability) of the microstructures.

Han et al. used microstereolithography (PμSL) to obtain very thin hydrogel structures that can act as microgrippers (Figure 4b).^[74] Similar to conventional stereolithography, PμSL is based on UV photopolymerization, which is used to fabricate 3D structures layer-by-layer. While stereolithography uses masks to illuminate each consecutive layer in parallel, PμSL uses a digital micromirror device with reconfigurable digital photo masks that can be easily changed to different patterns for each layer. In a typical PμSL process, the target object is drawn by computer-aided design (CAD) software. Using this CAD model, the 3D structures are sliced into 2D digital patterns, which are then transferred one by one to the digital micromirror device. This device modulates the local light intensity to which the resin is exposed.^[76,77] In the work by Han et al., pillars with a higher cross-linking density at the outside than at the inside of the gripper were printed from thermoresponsive PNIPAM. These different domains were encoded as gray-white bitmap images in the CAD model of the gripper, and the polymer resin was illuminated from these 2D bitmap images. This resulted in higher illumination intensities (i.e., more cross-linking) in

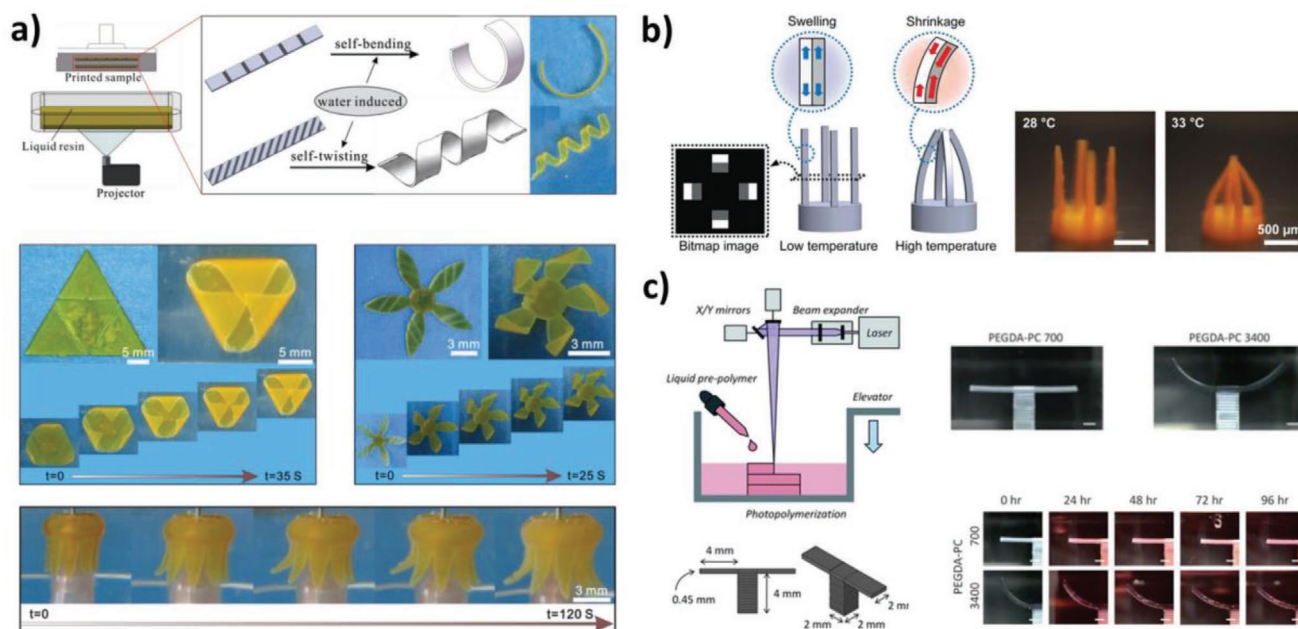


Figure 4. Stereolithography 3D printed hydrogel actuators: a) Hydrogel strips containing high-resolution microstructures with directional anisotropy, printed from a mixture of polyethylene glycol diacrylate (PEGDA), 2-hydroxyethyl methacrylate (HEMA), 2-(2-methoxyethoxy) ethyl methacrylate (MEO₂MA), aliphatic urethane diacrylate (AUD) and 3-sulfopropyl methacrylate potassium salt (SPMA). Shape deformations including bending and twisting could be induced by humidity or temperature changes. Reproduced with permission.^[73] Copyright 2019, Wiley-VCH. b) Microgrippers obtained by stereolithography 3D printing. Bending, and thereby closing of the gripper, was induced by a temperature change. Reproduced with permission.^[74] Copyright 2018, Springer Nature Ltd. c) Multicomponent hydrogel cantilever made from PEGDA and an acrylate-PEG-collagen (PC) mixture obtained by stereolithography 3D printing. Freestanding cantilevers with different elastic moduli, depending on the molecular mass of the PEGDA type used, were obtained. Cardiomyocyte cells seeded on the upper face of the cantilever create tensile stress along the cantilever surface and thus caused bending of the cantilever with the lower elastic modulus (PEGDA-PC 3400), but not of the stiffer cantilever (PEGDA-PC 700). Reproduced with permission.^[75] Copyright 2012, The Royal Society of Chemistry.

the “white” pixels of the bitmap at the outside of each pillar, i.e., the 3D printed material was stiffer at the outside. When heating the gripper above the LCST of PNIPAm, the domains with the lower cross-linking density at the inside would contract more strongly, which induced bending and thus closing of the gripper device.^[74] Thus, stereolithography 3D printing is clearly the method of choice when there is a simultaneous need for precise local modification of the materials properties, and the fabrication of small-size actuators. In another example, small cantilevers with beam sizes of 2 mm width, 4 mm length, and 0.45 mm thickness were produced from a multicomponent hydrogel system based on PEGDA with different molecular weights, and a mixture of PEG, acrylate, and collagen (PC). To form the hydrogel, the multicomponent resin was copolymerized using stereolithography 3D printing (Figure 4c).^[75] Cantilevers obtained from PEGDA with a higher molecular mass (e.g., 3400 g mol⁻¹) had a lower cross-linking density, and were thus softer than cantilevers fabricated from low molecular mass PEGDA (with 700 g mol⁻¹). When the cardiomyocyte cells grown on the upper face of the different cantilever types contracted, they caused bending of the softer PEGDA-3400 cantilevers but could not change the shape of the stiffer PEGDA-700 based objects. Thus, such structures can be used to quantify low-level mechanical stresses.^[75]

2.2.4. Two-Photon and Multiphoton Laser Lithography 3D Printing

Two-photon lithography is a further variation of stereolithography, by which 3D printed structures with even higher resolution can be obtained. The light source of this technique is not a UV source, but a pulsed femtosecond laser operated in the visible or near-infrared range ($\approx 780\text{--}800$ nm), a range for which the resin used is transparent. However, due to the high intensity of the laser pulses, and the narrow focal volume used (≈ 60 nm), two (or more) photons are absorbed simultaneously on the same atom, so that similar chemical processes as in conventional UV photopolymerization are initiated, i.e., the UV reactive resin is polymerized. As the laser is moved through the resin, polymerization is only initiated in the focal volume, so that the target 3D structures are built up voxel-by-voxel.^[78–80] In Figure 5a, a microscale hydrogel actuator obtained by multiphoton lithography using a near-infrared (NIR) femtosecond laser is presented.^[81] This material designed by Xiong et al. was made from poly(acrylamide-*co*-2-acrylamido-2-methyl-1-propane sulfonic acid) (poly(AAm-AMPS)) hydrogels and consisted of a main body with 6 arms. From these, only two had a homogeneous cross-linking density, the other four were more strongly cross-linked on their right side than on their left side, which was achieved by varying the irradiation time of the individual voxels forming the arms.^[81] In a consequence of the anisotropic distribution of their cross-linking, these hydrogel arms would bend to the left when immersed into water (the higher the anisotropy, the larger the bending angle, Figure 5b). The homogeneously cross-linked cantilevers remained unbent. When immersed into aqueous NaCl solution, the bending direction was reversed (Figure 5c). As illustrated by this example, two- and multiphoton stereolithography 3D printing gives access to hydrogel actuator structures that are more than one order of

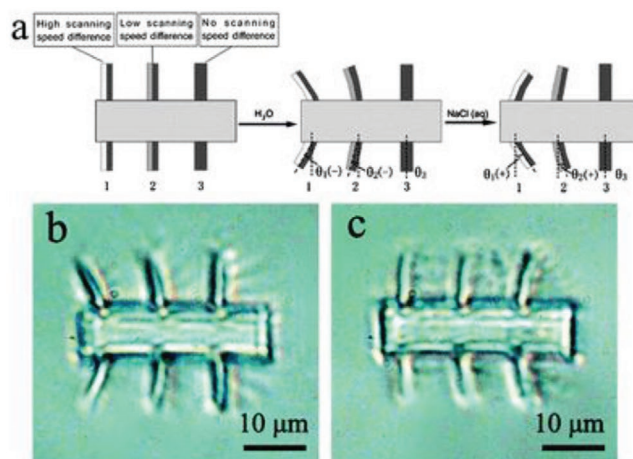


Figure 5. Multiphoton lithography 3D printed poly(acrylamide-*co*-2-acrylamido-2-methyl-1-propane sulfonic acid) (poly(AAm-AMPS)) hydrogel actuator with six microcantilever arms. a) Microcantilever arms 1 and 2 had different degrees of cross-linking on the right and left side, cantilever 3 was homogeneously cross-linked. This was achieved by varying the irradiation times along the cantilever arms. b) The thus created anisotropic microstructures 1 and 2 became bent when immersed into water, while the homogeneous cantilever 3 remained straight (from left to right: deformation angle -28.4° , -10.2° , and 0°). c) In aqueous NaCl solution, the effect was reversed (bending angle from left to right, 4.5° , 12.3° , and 16.2° , respectively). Reproduced with permission.^[81] Copyright 2011, The Royal Society of Chemistry.

magnitude smaller than the ones reported by conventional stereolithography 3D printing. Only few hydrogel actuators based on this technique were reported so far (possibly due to the high cost of such systems), so that the usefulness of this technique for the field cannot yet be fully appreciated.

3. Materials Aspects: Ink Formulation, Structural Integrity, and Stimulus Responsiveness

3.1. General Requirements on Inks for 3D Printing of Hydrogel Actuators: Ink and Precursor Formulation, and Interfacial Bonding

3.1.1. Polymer, Ink, and Precursor Formulation

From the above, it follows that progress in the field of 3D printed programmable actuators depends on three aspects: on the further development of the available instruments, on the clever design of the actuator structures, and on the availability of suitable precursors and inks for printing. As discussed in the previous section, most hydrogel actuators that have been reported in the literature so far were obtained by extrusion 3D printing, as these instruments are currently the most widespread ones in the academic sector. Therefore, the formulation of new materials for this sector is particularly important, yet also quite challenging. As discussed, suitable inks and molten filaments need to be shear-thinning and have a viscosity that is optimized for the size and geometry of the printing nozzle used, so that a molten or liquid fiber can be extruded without rupture. Additionally, the solidification, gelation, or formation

of other stabilizing structures of the extruded material (e.g., cross-links) need to be sufficiently fast to prevent deliquescence, or else the designated dimensions of the printed objects become distorted. Finally, as 3D printed objects are created voxel by voxel, it is essential that the inks used form sufficiently strong interfacial bonds between the deposited voxels in all directions (i.e., not only along the printed filament), so that the structural integrity of the final objects is not compromised.^[82] In the following, we will discuss how these requirements can be achieved.

The two types of materials used for extrusion 3D printing, polymer melts and polymer inks, typically differ widely in their rheological properties. To be suitable for this kind of processing, they must be shear-thinning and quickly recover their high viscosity state after the extrusion process. Polymer melts typically comply with both requirements due to their viscoelastic properties. In many cases, their viscosity is reduced by several orders of magnitude with an increasing shear rate. After the printing process, they rapidly recover the high viscosity state, and further harden during cooling and crystallization, so that the dimensions of the originally deposited voxel are not significantly distorted. Polymer inks used for 3D printing, on the other hand, are typically formulated from a mixture of solvent and precursors, including (macro)monomers, prepolymers, bifunctional or multifunctional cross-linkers. This yields low viscosity solutions which would deliquesce after the printing process, and which generally do not have shear-thinning properties. For this reason, so-called rheology modifiers are added. These are polymers or particles that form reversible molecular interactions with the other components of the ink (e.g., van-der-Waals or hydrogen bonds, dipolar or ionic interactions). Applying shear forces temporarily breaks many of these reversible intermolecular interactions, leads to a reduction of the local viscosity by orders of magnitude, and induces viscous flow.^[83] Commonly used rheology modifiers are triblock copolymers with hydrogen bond acceptors (e.g., Pluronic F127),^[32] hydrophilic nanoclays (e.g., laponite),^[84] and polymeric microparticles (e.g., from poly(acrylic acid)).^[85] With these additives, the printed objects maintain their shape, which is then locked in by post-treatment, e.g., UV cross-linking, so that the desired covalently connected polymer hydrogels are obtained with high shape fidelity. The optimization of the rheology modifier amount is performed by considering two essential rheological properties, which are the shear-thinning behavior and the shape fidelity of the ink. As discussed, shear-thinning hydrogel inks decrease in viscosity with increased shear stress. Viscoelastic material can be extruded from a nozzle if the shear stress is above its yield stress, which is the minimum stress value needed to induce viscoelastic flow of the ink ($G' > G''$). Under these conditions, the intermolecular interactions between the rheology modifier and the surrounding ink components are broken.

At too high concentrations of rheology modifier, strongly bound clusters form, which results in the noncontinuous flow of material and is the main reason for nozzle clogging. If dynamic cross-linked hydrogels are printed, their cross-links need to break by the applied shear stress, causing a transition from an elastic ($G' > G''$) to a viscous behavior ($G'' > G'$). A high shape fidelity is obtained if the high viscosity state is recovered sufficiently fast after removing the shear stress. This depends on the nature of

the intermolecular interactions of the rheology modifier with the other ink components.^[86,87] In the same way as the overall viscosity and shear thinning behavior of each system have to be optimized separately, so the optimal amount of rheology modifier has to be determined experimentally and depends on the additive type. The minimum amounts for commonly used rheology modifiers reported in the literature are: 18% w/v for Pluronic F-127, 5% w/v for nanoclay, and 0.5% w/v for carbomer microgels.^[85] Although rheology modifiers enhance the 3D printability of hydrogels, they affect the resulting materials properties, and therefore the use of an optimal amount (as much as needed, as little as possible) is crucial. For example, the mechanical properties of hydrogels containing charged laponite are poor when the content of these nanoparticles is too high.^[88]

Besides covalently cross-linked polymer networks, there are also polymer hydrogels that are based on a dynamic network structure. Such networks are connected by reversible covalent bonds, and they can be directly printed from inks containing the final chemical structures of their scaffolds. When shear forces are applied to the networks during printing, the dynamic covalent bonds are broken, and the network undergoes a transition from the elastic to the viscous state, which allows for extrusion printing. Due to the reversibility of dynamic covalent bond formation, the dynamic network structure is re-formed after the printing process. For such systems, it is crucial that the rate by which the dynamic bonds reform is sufficiently fast, so that the printed voxels retain their shape.^[89] In principle, such dynamics networks can be obtained by any kind of interaction that is reversible and sufficiently strong. Dynamic covalent bonds containing heteroatoms are particularly interesting in the context of 3D printing as they meet these criteria. Unlike conventional carbon-carbon bonds, which can be considered as static, these carbon-heteroatom bonds undergo continuous bonding-debonding transitions at a rate that is fast enough for immediate bond recovery once the shear forces experienced during printing are removed.^[90] Examples for such dynamic functional groups are imines (including Schiff's base), hydrazones, and Diels-Alder reaction adducts.^[55] For example, Wang et al. obtained shear-thinning 3D printable inks for hyaluronic acid hydrogels by functionalizing the starting materials with hydrazide and aldehyde residues (**Figure 6a**).^[91] It was shown that the hydrazone cross-linkers induced high shape fidelity in the multilayer materials that were printed; also filament flow over time was prevented.

Dynamic cross-linking can also be implemented by physical intermolecular interactions, including hydrogen bonds,^[91] hydrophobic,^[92] ionic,^[45] and supramolecular host-guest interactions.^[93] As these interactions are typically weaker than a corresponding amount of covalent bonds, they can also be temporarily broken when shear forces are applied, and undergo shear-thinning when printed (**Figure 6b**). Additionally, such physical interactions, e.g., complexation between oppositely charged polymers,^[94] can lead to improved printing resolution. This was observed when negatively charged hyaluronic acid methacrylate (HAMA) hydrogels underwent complexation with cationic chitosan.^[94]

As 3D printed objects are fabricated voxel by voxel, the interaction strength of adjacent voxels that were not printed along the same filament strand is of great significance for the stability of the target object, especially if it is subject to persistent mechanical loads. If this interaction between the neighboring

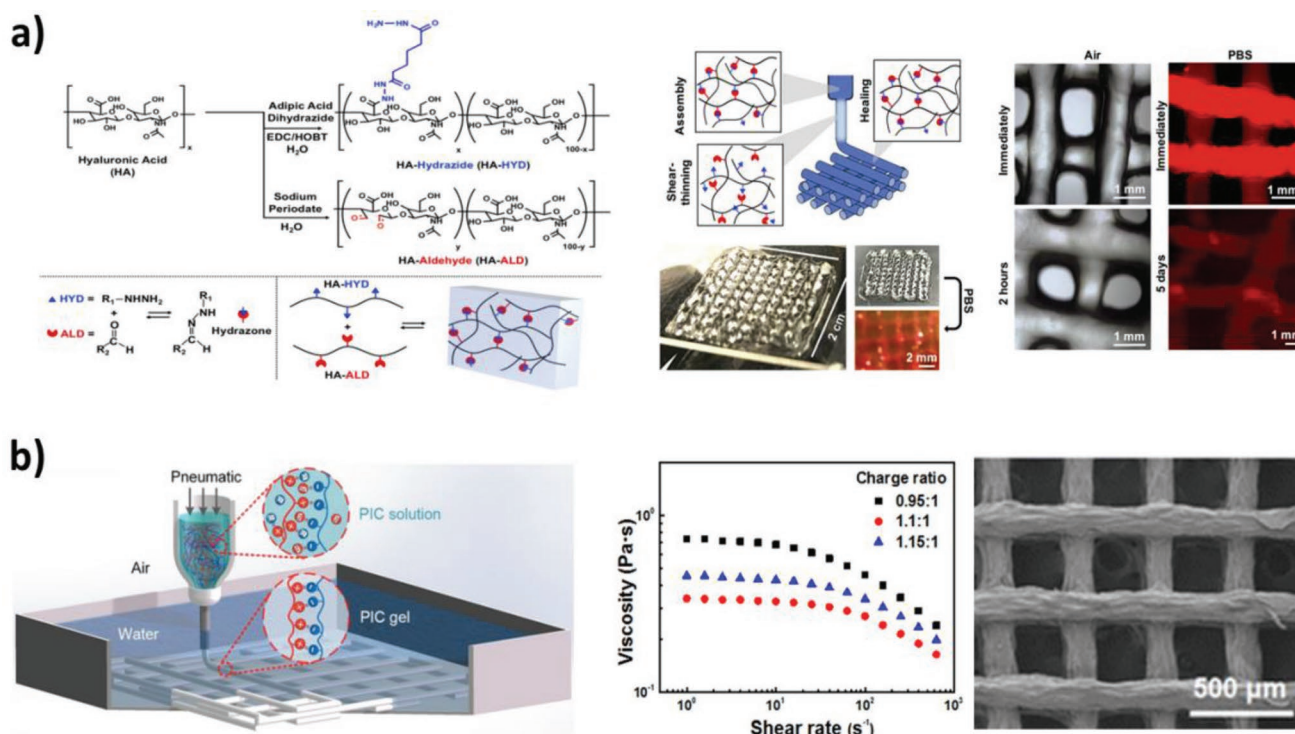


Figure 6. Examples of shear-thinning 3D printed hydrogels that are stabilized by dynamic covalent bonds and dynamic physical interactions: a) Hydrogel cross-linking by dynamic hydrazone bonds, which were obtained from precursors with hydrazide and aldehyde groups. The material is shear-thinning due to the reversibility of the hydrazone bond. Reproduced with permission.^[91] Copyright 2018, Wiley-VCH. b) Physically cross-linked polyelectrolyte hydrogel formed from poly(sodium-*p*-styrene sulfonate) and poly(3-(methacryloylamino)-propyl-trimethylammonium chloride). The shear-thinning of the polyelectrolyte complex depended on the ratio of the two components and could be further controlled by temperature. Reproduced with permission.^[45] Copyright 2016, American Chemical Society.

voxels—either through adhesive or chemical interactions—is not sufficiently strong, the printed layers will delaminate. This is particularly relevant in the context of 3D printing of hydrogels actuators due to the internal stress they encounter during swelling and actuation.^[47] For example, bending hydrogel bilayers based on materials with different swelling ratios can only be realized if their two layers are strongly connected at the interface.^[95] With strong bonding at that interfaces, hydrogel actuators can undergo repeatable and fast actuation.^[36] The same strategies that can be applied to connect and/or cross-link bulk hydrogels can be used to overcome delamination of adjacent voxels or layers of 3D printed hydrogels. Examples are the UV cross-linkers, reinforcement by nanofillers, use of oppositely charged polymers, and the formation of interpenetrating polymer networks (IPNs). Stabilization by UV cross-linking has been discussed above. Nanofillers are particles with a large surface area and a high density of functional groups. These can be used to obtain physical or covalent bonds between adjacent hydrogel voxels or layers. As a typical example, laponite nanoclay was used as a filler in a hydrogel bilayer which could sustain bending stresses and undergo reversible actuation without delamination.^[96] Without nanoclay, such structures were shown to delaminate. For example, it was shown that the bilayer PNIPAm-PNAGA hydrogel without laponite nanoclays easily delaminated after two bending cycles.^[96] Electrostatic interactions between oppositely charged polyelectrolyte building blocks also lead to strong interfacial bonding. Oppositely charged hydrogel layers form strong polyelectrolyte com-

plexes on the molecular level, which creates adhesive forces. This strategy to compatibilize different components at interfaces is found in natural actuators containing charged polysaccharides.^[95]

Formation of IPNs is a strategy that slightly differs from the above-introduced approaches. Instead of directly introducing bonding interactions at the interface of different hydrogel building blocks, a second kind of network is formed around them. For that purpose, the printed components (forming the first network, e.g. a dynamic covalent network) are swollen with the designated monomer for the second network, followed by cross-linking. This is easily achieved due to the high swellability of hydrogels in monomers with matching hydrophilicity. During the following polymerization step, the newly formed polymer chains penetrate the first polymer network, so that interpenetrating networks are obtained. Thus, the high mechanical strength typically found in IPNs is the result of irreversible molecular entanglement of the two networks.^[97] Additional specific intermolecular interactions (e.g., hydrogen bonds) may further enhance the effect.^[98]

3.2. 3D Printed Programmable Hydrogel Actuators

3.2.1. Programming Actuation

As demonstrated by the examples in Section 2, hydrogel actuators can undergo simple or reversible shape transformations

when exposed to suitable external stimuli. The exact type of actuation as well as its magnitude can be programmed into the hydrogel by combining the stimulus-responsive, active components with the elastic resorting forces provided by the hydrogel matrix during 3D printing and post-treatment. In some cases, the hydrogel matrix itself can also be a stimulus-responsive component, e.g. when polymers with an LCST or pH-responsive groups are used. Simple types of actuators (e.g., bilayers that undergo one-way bending) are easily achieved even without the need for 3D printing (for example by solvent-casting polymer hydrogel bilayers with different degrees of cross-linking onto each other). However, complex programmed actuation modes as found in nature require more sophisticated structuring, often with anisotropy in more than one dimension. To some extent, this can be achieved by self-assembled systems or microfabrication techniques (especially when targeting flat systems), yet for more complex objects, 3D printing is unrivaled in the degree of flexibility it provides to the fabrication process. Yet a process is only as versatile as the family of materials that can be processed by it, and the more materials with different kinds of programmable actuation become available, the more advanced the function of the accessible structures will be. In this chapter, we will therefore focus on the different kinds of active components that can be used for actuation. These are either the polymer networks themselves, or additives with special properties, for example, ferromagnetism.

3.2.2. 3D Printed Thermoresponsive Hydrogel Actuators

Thermoresponsive polymers undergo changes in their molecular conformation when their solutions are either cooled or heated. Hydrogels synthesized from such polymers can be actuated by temperature changes, as the conformational changes affect the state of swelling/de-swelling of the hydrogel. Two opposite types of thermoresponsive polymers have been reported. Polymers with a lower critical solution temperature (LCST) undergo a coil-to-globule transition as their temperature is increased above the LCST. A well-known example for such a polymer is poly(*N*-isopropylacrylamide) (PNIPAm),^[99] which was discussed in the previous chapters of this work. The coil-to-globule transition of PNIPAm is an aggregation of polymer chains above the LCST that is driven by different intramolecular processes, including the breakdown of the hydrogen bond network between the water molecules surrounding the hydrophobic isopropyl groups, the perturbation of the hydrogen bonds between water and the PNIPAm amide residues, and a decrease in the level of organization of the water molecules that surround the polymer chains.^[100] The LCST transition causes a collapse of the entire hydrogel, i.e., a drastic decrease in the swellability of the hydrogel is observed. Thus, when PNIPAm strips are attached to another material that does not undergo a LCST transition, the internal stresses induced in the bilayer lead to bending.^[101] The second kind of thermoresponsiveness found in polymers is an upper critical solution temperature (UCST),^[18] which can be explained by the Flory-Huggins-theory.^[102] Below the UCST, polymer chains are collapsed due to preferred polymer–polymer interaction, while polymer–solvent interactions are preferred above the

UCST. While enhanced solubility with increasing temperature is a common feature in most polymers, the effect is particularly pronounced in those with an UCST. PNIPAm hydrogels are the most widespread LCST hydrogels.^[99] They undergo a fast phase transition and water release above ≈ 32 °C. Their coil-to-globule transition is followed by water release and the hydrogel stiffens in consequence of polymer chain aggregation and an overall higher polymer to water ratio in the collapsed gel. PNIPAm hydrogels are frequently used as soft actuators in the biomedical field, as they have a relatively fast response and their LCST is near human body temperature.^[103] The 3D printability of PNIPAm hydrogels and their programmable actuation have been investigated in several studies. In one example, stereolithography 3D printing was used. In this study, the degree of cross-linking and the chemical composition (by copolymerization of *N*-isopropylacrylamide and 2-carboxyethylacrylate) were varied, and different kinds of surface structures were produced (Figure 1a).^[34] Thermoresponsive materials with a high deformation rate (up to 1.55 cm in 15 min) were obtained by using hydrogels with a high surface area to volume ratio. A gradient in the degree of cross-linking affected the local swellability of the material, and a gradient in the molar fraction of poly(2-carboxyethylacrylate) repeat units contributed to pH responsiveness in addition to the thermo-responsive behavior. Liu et al. designed 3D printed bioinspired tubes, whose actuation mimics buckling (as observed in the saguaro cactus after rainfall, Figure 7a).^[104] The tubes were printed vertically by 3D extrusion printing and contained strips of soft swellable PNIPAm and stiff non-swellable PAAm arranged parallel to the tube axis. When the tube was immersed in water at high temperature (e.g., 50 °C), the PNIPAm stripes collapsed, which created compressive axial stresses at the PNIPAm–PAAm interface. At $T < \text{LCST}$, the swelling of PNIPAm was constrained on both sides by the passive PAAm strips, which created a swelling mismatch, together with compressive stresses, and induced buckling of the structure. The swelling mismatch approach was also used to fabricate hydrogel actuators that could open and close in response to temperature changes. For this, a hydrogel was extrusion 3D printed from thermoresponsive PNIPAm and non-responsive poly(2-hydroxyethyl methacrylate) (poly(HEMA)) networks, to which a polyurethane-based material containing poly(ethylene oxide) segments (PEO-PU) had been added (Figure 7b).^[105] The hydrogel had the shape of a flatplan for a 3D cube, with PNIPAm in the folding lines, and poly(HEMA) in the remainder of the structure. Above the LCST, the PNIPAm sections contracted, so that the flatplan folded up into a 3D hollow box due to the build-up of internal stresses in the folding lines. Chen et al. demonstrated how 3D printing can be combined with more conventional polymer processing technologies like electrospinning.^[106] Electrospun polymer membranes offer great potential for fast actuation due to their high porosity. However, they cannot be directly used for actuation, as their fiber orientation is random. To benefit from the properties of both kinds of materials, PNIPAm/clay composites were printed on electrospun PNIPAm hydrogels (Figure 7c). When the temperature was increased above the LCST of PNIPAm, a swellability mismatch between the 3D printed PNIPAm/clay

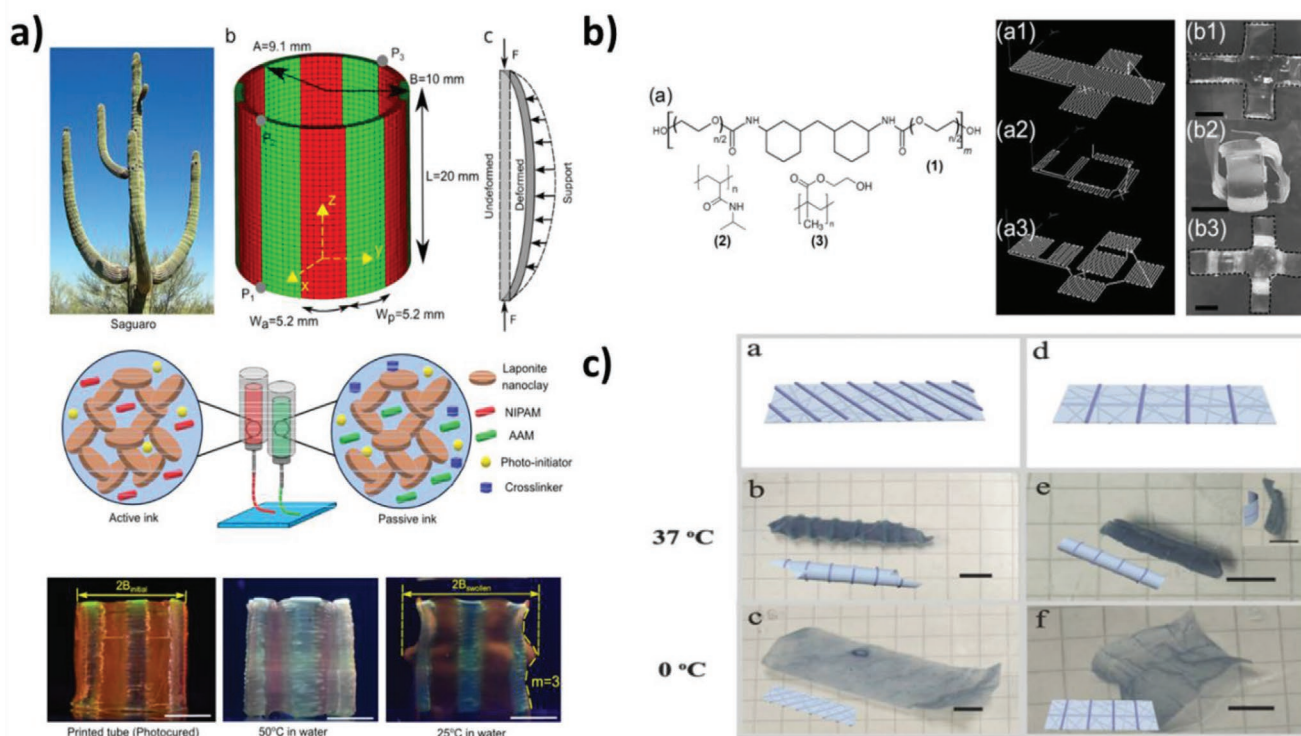


Figure 7. Thermoresponsive 3D printed hydrogel actuators: a) Hydrogel tube made from thermoresponsive PNIPAm and inactive polyacrylamide (PAAm) strips. The tube structure imitates the Saguaro cactus morphology. At $T > LCST$, the PNIPAm strips collapse and experience axial stress. At $T < LCST$, the swollen PNIPAm stripes become softer, so that buckling in the PNIPAm region is observed, while the material is stabilized by the PAAm parts. Reproduced with permission.^[104] Copyright 2019, Elsevier. b) Flatplan for a 3D cube formed PNIPAm and poly(HEMA) hydrogel patches which have been modified with a polyurethane-containing poly(ethylene oxide) segments. The thermoresponsive PNIPAm patches at the folding edges contract above the LCST, so that the flatplan folds to form the 3D cube. Reproduced with permission.^[105] Copyright 2016, Wiley-VCH. c) Combination of conventional electrospinning with 3D printing: patterns of PNIPAm/clay composites were printed onto electrospun PNIPAm hydrogels. Depending on the printing direction, different shape changes (e.g., rolling, bending, and reopening) were programmed. The actuation was reversible when changing the temperature from 37 °C to 0 °C. Reproduced with permission.^[106] Copyright 2018, Wiley-VCH.

patterns and the electrospun material was observed, and the internal stress thus created caused rolling or bending. The effect could be reversed at reduced temperature. This kind of actuation mimics the stimuli-induced morphogenetic transitions of planar sheets in biological materials.^[106]

In contrast to LCST materials, UCST hydrogels show a positive thermorespons, i.e., their hydration and swelling increase strongly above the UCST. UCST polymers, such as poly(acrylamide-co-acrylic acid) (poly(AAm-co-AAc)),^[107] poly(acrylamide-co-acrylonitrile) poly(AAm-co-AN),^[108] or poly(*N*-acryloyl glycinamide) (PNAGA), have strong hydrogen bonds between the polymer chains.^[109] With increasing thermal energy of the system, these bonds are broken, which further enhances the hydrogel swelling. The formulation of inks for 3D printing of UCST hydrogels remains a challenge, since ink additives such as rheology modifiers also affect the hydrogen bond network, and in consequence, the UCST nature is often lost. While hydrogel bilayer actuators (obtained by other processing techniques) with one UCST component have been reported in the literature,^[18,23,96] to the best of our knowledge, UCST-based 3D printed hydrogel actuators have not been reported yet.

3.2.3. 3D Printed Electroactive and Ion Conductive Hydrogel Actuators

Triggering actuation with electric fields is advantageous, as it allows a fast stimulation and control over the amplitude of the material response. Materials designed to respond to electric stimulation need to have either a high intrinsic electron conductivity (e.g., polypyrrole or polyaniline), contain conductive fillers,^[110] or have a high charge carrier mobility that enables ionic conductivity. The latter is easily achieved in polyelectrolyte hydrogels which have a high water content and charge carrier density.^[111] Han et al. synthesized ion conductive 3D printed polyelectrolyte hydrogels by copolymerization of acrylic acid with poly(ethylene glycol) diacrylate (PEGDA) (Figure 8a).^[112] When the thus obtained electroactive hydrogel (EAH) was immersed into an electrolyte solution (e.g., phosphate-buffered saline), the carboxylic groups deprotonated, so that a negatively charged polymer network with a high amount of mobile cationic counterions was generated. The high counterion content is the physical origin of the osmotic pressure that builds up between the electrolyte solution and the polymer network, which is compensated by water uptake. When exposed to the static electric

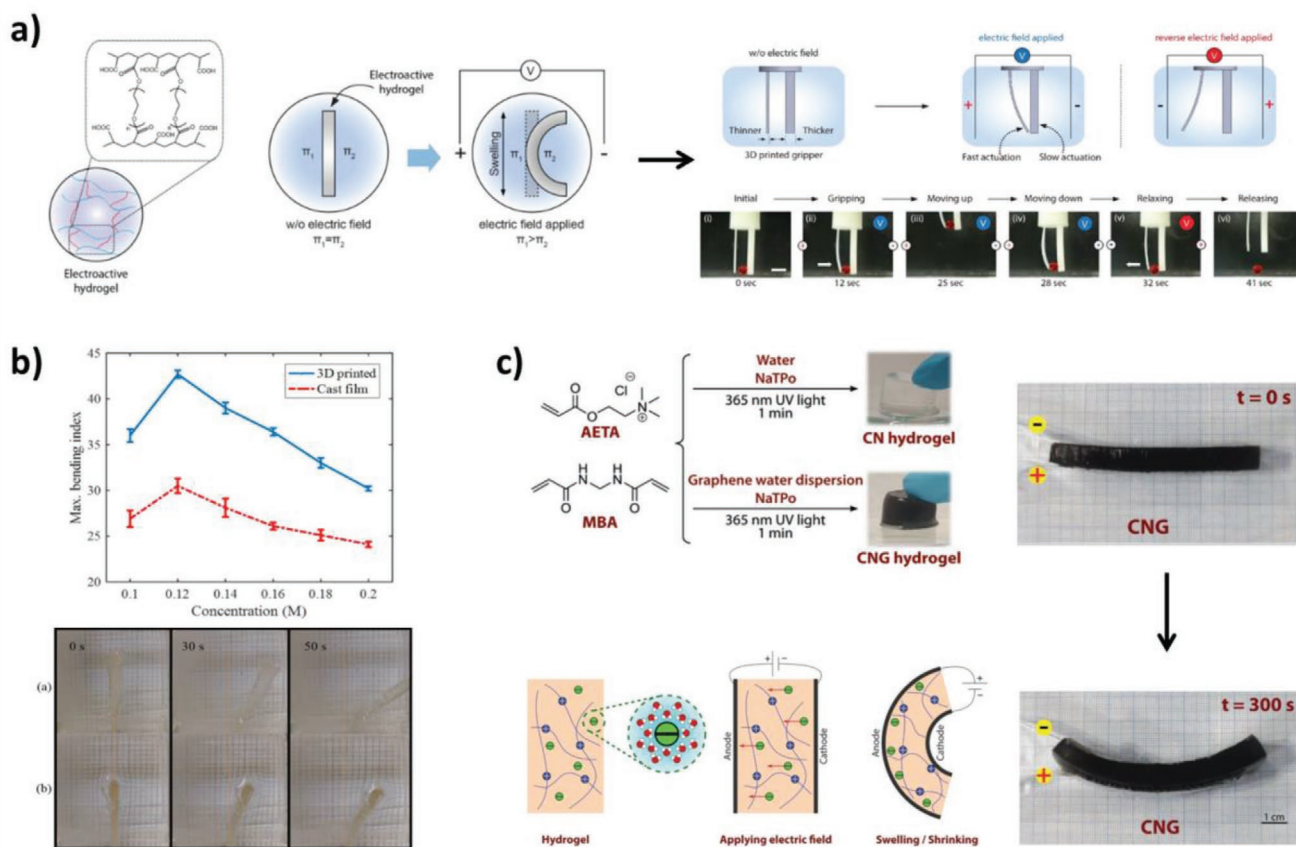


Figure 8. Examples of 3D printed electroactive hydrogel actuators. a) Hydrogels obtained from poly(acrylic acid)-*co*-(ethylene glycol diacrylate) were swollen in an electrolyte solution and actuated by an electric field. This induced a charge gradient across the material and led to bending. The obtained gradient, and thus the curvature of the material, depended on the hydrogel thickness. Using hydrogel strips with different thickness, a 3D printed gripper was obtained. When the field was switched on, the thin strip was deformed and pressed against the thick strip, and reopened when the field direction was changed. Reproduced with permission.^[112] Copyright 2018, American Chemical Society b) Comparison of electroactive chitosan hydrogels obtained by solvent-casting and 3D printing. The gels built up a charge-density gradient within an electric field, as in (a). The 3D printed gel had a higher surface to volume ratio and thus could build up a stronger charge gradient, leading to more bending. Reproduced with permission.^[113] Copyright 2017, Elsevier. c) Electron conductive hydrogels made from (2-(acryloyloxy)-ethyl)-trimethylammonium (AETA), *N,N'*-methylenebisacrylamide (MBA) and conductive graphene bent when applying a DC potential. Reproduced with permission.^[115] Copyright 2020, Wiley-VCH.

field between two electrodes, the cations in the solution surrounding the hydrogel start to migrate towards the cathode, which causes a cation gradient in the solution. This imbalance affects the osmotic pressure of the EAH, and thus its local degree of swelling. An increase or decrease in swelling on one side of the gel can cause bending of the hydrogel towards the cathode. This actuation could be controlled either by changing the electrolyte concentration or the electric field strength.^[112] In a similar study, the effect of the hydrogel thickness on the degree of bending of EAHs was studied. Finger-like hydrogel actuators with two different thicknesses were printed, as shown in Figure 8a (left: 0.25 mm, right: 1 mm). While the thin finger bent towards the thick one in the presence of the electric field, the thick finger itself remained straight, so that the material formed a simple gripper which could pick up and release a small plastic sphere.^[112] Zolfagharian et al. 3D printed ionic, pH-responsive chitosan hydrogels and compared them with similar materials obtained by solvent casting (Figure 8b).^[113] At the same electric field strength, the 3D printed hydrogel could

be actuated more strongly than the solvent cast material. Apparently, the surface to volume ratio of the 3D printed hydrogel was higher, which also affected the diffusivity of the ions. By carefully designing the geometry of electroactive hydrogels, their response can be further enhanced. For example, 3D printed hydrogels consisting of grid-like structures would bend more easily than bulk structures with the same dimensions in the presence of an electric field.^[114] Electron conductive 3D printed hydrogels have been obtained by adding conductive graphene as filler to a polycationic acrylate/alginate-based hydrogel. This additive also enhanced the mechanical stability of the materials, as described by López-Díaz et al. (Figure 8c).^[115] In contrast to the above-described gels whose actuation was based on ionic conductivity and thus required an aqueous environment, this material possessed intrinsic conductivity and could thus be actuated in the absence of water. Likewise, it only required a low potential for actuation. Electron-conductive polymers (sometimes also called electroactive polymers) can be actuated because they change their molecular volume when a voltage

is applied, i.e., they extend or contract. This is a direct result of changes in their charge density. At high charge density, like charges repel each other so that the material expands while the material contracts back into its equilibrium dimensions at a lower charge density. The effect may be increased when it is accompanied with in- and out flux of water with changes in the charge density of the material.

3.2.4. 3D Printed Magneto-responsive Hydrogel Actuators

Magnetic fields can be used to actuate ferromagnetic materials fast and with precise spatiotemporal control. Ferromagnetic hydrogels are typically obtained by incorporating ferromagnetic particles into a cross-linked polymer network. Previously reported 3D printable hydrogel actuators mainly contained ferromagnetic $\gamma\text{-Fe}_2\text{O}_3$, Fe_3O_4 , or CoFe_2O_4 particles. For a detailed discussion about the synthesis of magnetic hydrogels, we refer to the review paper by Li et al.^[116] It is well known for ferromagnetic materials that the orientation of the magnetic moments of the building blocks affects the overall magnetic properties of the material. Thus, the alignment of the magnetic

particles during printing is crucial. Anisotropic alignment can also be induced by 3D printing if the particles themselves possess an anisotropic shape.^[117] Podstawczyk et al. incorporated magneto-responsive iron oxide nanoparticles functionalized with polyacrylic acid (PAA) into alginate-methylcellulose hydrogels. These hydrogel actuators had square and honeycomb grid structures with varied mesh sizes. The surface functionalization of the magnetic nanoparticles with PAA improved the rheological properties of the ink, ensured their alignment and contributed to mechanical stabilization of the gel by intramolecular cross-linking (Figure 9a).^[118] The extent of actuation obtained in the presence of the magnetic field did not depend on the grid shape, but on the ratio of filled and void voxels (the so-called infill ratio). Another effective way to align the magnetic fillers of hydrogels is applying an external magnetic field during the fabrication process. This strategy was used to produce magneto-responsive actuators that mimic the motion of worms and cilia (Figure 9b).^[119] Cilia-like pillar arrays were 3D printed in the presence of an external magnet, whose orientation was changed during printing, so that the pillars differed in the orientation of their magnetic particles, and thus in their bending direction. When actuated by a

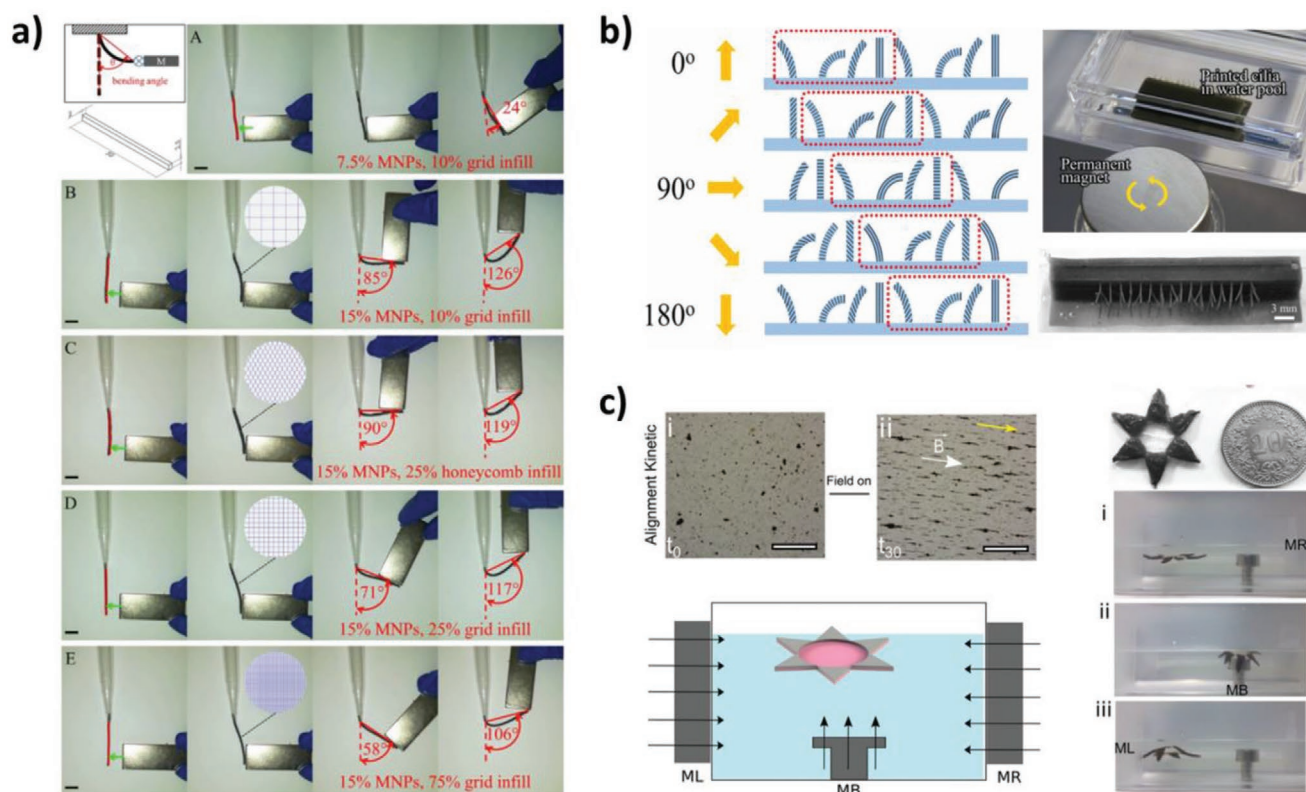


Figure 9. 3D printed magneto-responsive actuators: a) Hydrogels made from alginate, methylcellulose, and poly(acrylic acid)-functionalized magnetic nanoparticles. The accessible modes of actuation obtained with different geometries of the printed grid structure (square or honeycomb), and different ratios of filled and void voxels (infill ratio) were tested. An increase in the infill ratio decreased the degree of bending of the hydrogel, while no significant difference was found between square and honeycomb structures. Reproduced with permission.^[118] Copyright 2020, Elsevier. b) Cilia-inspired 3D printed magneto-responsive pillar arrays made from poly(urethane-co-acrylate) and carbonyl iron powder. The iron microparticles were anisotropically aligned by an external magnetic field at different angles during printing. Applying a rotating magnetic field induced a site-specific amount of pillar bending in the array. Reproduced with permission.^[119] Copyright 2019, IOP Publishing. c) Hydrogel made from gelatin, poly(acrylate), and iron nanoparticles. The particles were aligned during the printing process by a magnetic field, so that the printed star-fish-shaped actuator could (i) swim (ii) wrap around a target, and (iii) swim back. Reproduced with permission.^[120] Copyright 2019, Wiley-VCH.

rotating magnet after printing, their collective response was not in phase, but wave-like, which is similar to the movement of worms, or the motion of natural cilia when transporting mucus across tissues.

Tognato et al. reported 3D printed magneto-responsive gelatin-poly(acrylate) hydrogels that contained iron nanoparticles (Figure 9c).^[120] The nanoparticles were anisotropically aligned by a magnetic field while extrusion 3D printing starfish-shaped hydrogels. The actuator consisted of a bilayer, where the orientation and distribution of the particles in each layer differed. The thus obtained hydrogel showed complex shape deformations, including bending, wrapping around a magnetic target, and swimming in aqueous environment in response to changes in the magnetic field used for actuation.

3.2.5. 3D Printed Humidity Responsive Hydrogel Actuator

Several organisms have developed the ability to adapt themselves to external humidity fluctuations, as discussed in the introduction. This is typically achieved by bending in response to relatively small amount of water uptake.^[121] Inspired by pine cone bilayer structure, researchers fabricated 3D printed composites from carbon fibers embedded into a moisture-responsive polyamide matrix (PA6, Figure 10a).^[122] By 3D printing, hydrogel system with up to three layers could be obtained, each with a different orientation (e.g., 45°, 90°, and -45°). The moisture uptake induced internal stresses and triggered reversible bending.

In another study, humidity-responsive hydrogels were used to mimic actuation found in natural microstructures. For this aim, a PEGDA hydrogel with microsized openings was fabricated by femtosecond laser direct writing (Figure 10b).^[123] The structures were printed in the shape of a plant stomata, which could open and close in response to humidity changes by swelling. The responsiveness could be modulated through the cross-linking density of the material and was reversible. 3D printed microcantilevers could also be actuated by humidity changes. These materials consisted of swelling PEGDA segments and hydrophobic poly(butyl methacrylate) (BMA) segments. When swollen in water vapor, the PEGDA segments bent and thus caused a shape change of the entire cantilever.

4. Conclusion

The above-presented examples illustrate how programmable actuation can be achieved by an ingenious combination of 3D printing approaches, stimulus-responsive polymers, and creative material designs. Compared to conventional polymer and hydrogel processing techniques, 3D printing techniques give access to highly customized and precisely processed actuator prototypes in one or only few processing steps. The design flexibility that these techniques provide is unrivaled, and the palette of suitable actuator materials to choose from is ever-increasing with ongoing research.

On the other hand, a number of challenges in 3D printing of hydrogel actuators still have to be addressed. Currently,

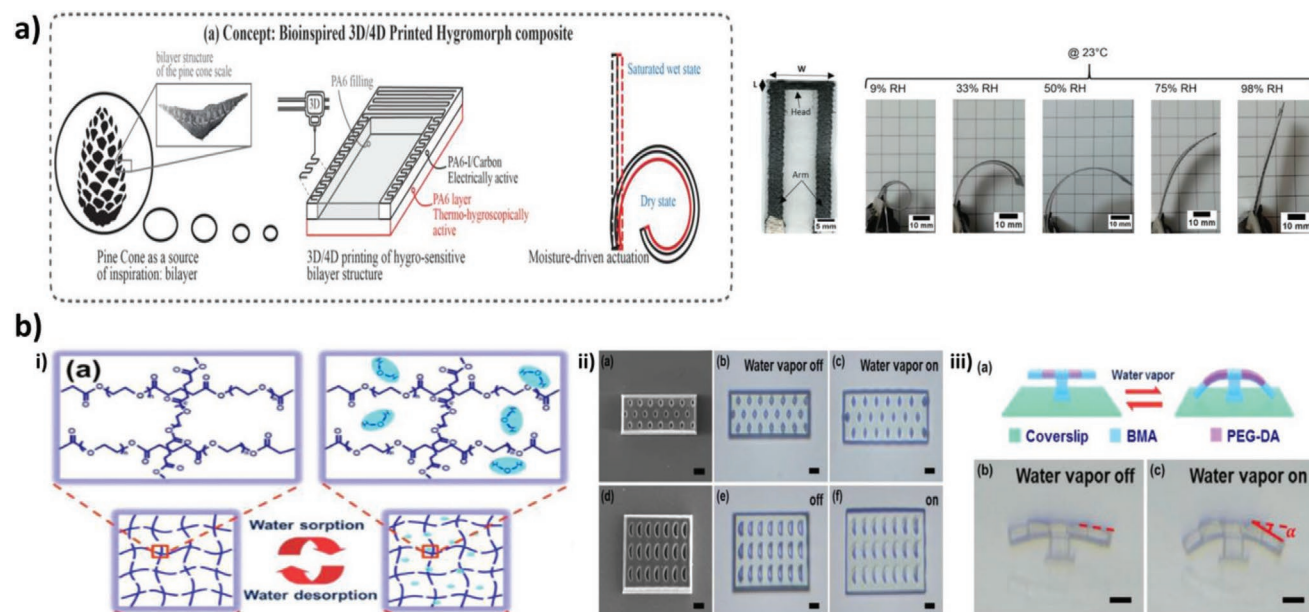


Figure 10. 3D printed humidity-responsive hydrogel actuators: a) Pine cone-inspired bilayer hydrogel made from polyamide (PA6) and poly hexamethylene isophthalamide (PA6-I)/Carbon layers by extrusion 3D printing. PA6 hydrogels absorbed humidity from the environment, and the carbon fillers made the system electron conductive. The hydrogel system was able to undergo shape transitions from the rolled (9% humidity) to the opened state (98% humidity). Reproduced with permission.^[122] Copyright 2019, Wiley-VCH. b-i) Humidity-responsive poly(ethylene glycol) diacrylate (PEGDA) hydrogels increase in size in the presence of water; ii) Stomata-inspired structures printed from this material which could open and close their pores in response to changes of the local humidity; iii) Actuator consisting of PEGDA segments and poly(butyl methacrylate) (BMA) strips. The PEGDA domains swelled in the presence of water vapor and were softened, which caused overall bending of the actuator. Reproduced with permission.^[123] Copyright 2018, Elsevier.

most of the hydrogel actuators are printed by extrusion 3D printing, which requires rheology modifiers that often yield polymer networks with poorer mechanical properties. This limits the force and energy the printed actuator can provide, and thus its possible applications. Thus, the design and synthesis of system-specific rheology modifiers that rather enhance than reduce the performance of hydrogel actuators are required.

Another current limitation of the family of 3D printing techniques is its resolution, which is currently in the range of tens to hundred of micrometers. This yields printed structures on the millimeter to centimeter scale. The biomedical field would certainly benefit from a further miniaturization of the printing techniques, so that structures in the sub-millimeter range, or even smaller, could be realized, for example as sensor–actuator combinations in implants that autonomously and locally deliver drugs.

While programmable actuation has been demonstrated using a number of external stimuli, this is still confined to simple types of motion, and complex actuation is only obtained in exceptional cases, such as in the example of the swimming star fish (Figure 9). In nature, more complex actuation is obtained by coupling different structural and compositional features, such as anisotropic alignment of constituents, multiple material components, and gradients in the material composition. The current 3D printed hydrogels mostly utilize one of the above-mentioned features to achieve actuation; however, more complex combinations need to be studied in order to obtain more complex, life-like and autonomous actuation. We define such complex actuation as the ability to not only arbitrarily control shape changes, but to also precisely tune and time them, so that the obtained actuators can deliver the required mechanical output at the desired time. For this, one would require basic “building blocks” whose amount of motion per unit volume is quantified. Once these are available, simulation tools that combine such building blocks could be developed and used to predict in which way the blocks have to be combined to obtain the desired actuator output. In addition to that, one further open question in the field is how to program sequences of motion, or to remotely control hydrogel-based actuators. For example, it is not yet possible to design an actuator that can swim and change its direction on demand. Electronic remote control should be avoided, as it is difficult to establish in an aqueous environment. Other suitable platforms for remotely guiding or stimulating hydrogel actuators would be light or magnetic fields, which would enable precisely timed interaction with the material.

Achieving such progress will depend on continuing improvements in the printing hardware (e.g., better resolutions with higher repeatability), a more detailed understanding of the fine structure of complex natural actuators in order to inspire the design of more complex 3D printed actuators, and the development of stimulus-responsive inks and precursors that give access to materials with stronger, faster, and reliable actuation. We believe that further improvements in these fields will give access to ever more sophisticated programmed actuators with a robustness that makes them useful appliances in soft electronics, robotics, and the biomedical field.

Acknowledgements

This work was supported by funding from Saarland University. Open access funding enabled and organized by Projekt DEAL.

Conflict of Interest

The authors declare no conflict of interest.

Keywords

3D printing, actuations, polymer hydrogels, stimulus-responsive polymers

Received: May 10, 2022

Revised: June 22, 2022

Published online: July 24, 2022

- [1] Y. Wang, *Biomaterials* **2018**, *178*, 663.
- [2] I. Burgert, P. Fratzl, *Philos. Trans. R. Soc., A* **2009**, *367*, 1541.
- [3] H. Quan, D. Kisailus, M. A. Meyers, *Nat. Rev. Mater.* **2021**, *6*, 264.
- [4] R. M. Erb, J. S. Sander, R. Grisch, A. R. Studart, *Nat. Commun.* **2013**, *4*, 1712.
- [5] A. L. e Duigou, M. Castro, *Sci. Rep.* **2016**, *6*, 18105.
- [6] A. R. Studart, R. M. Erb, *Soft Matter* **2014**, *10*, 1284.
- [7] L. Zhang, S. Chizhik, Y. Wen, P. Naumov, *Adv. Funct. Mater.* **2016**, *26*, 1040.
- [8] Y. Yang, Y. Wu, C. Li, X. Yang, W. Chen, *Adv. Intell. Syst.* **2020**, *2*, 1900077.
- [9] M. Wang, B.-P. Lin, H. Yang, *Nat. Commun.* **2016**, *7*, 13981.
- [10] J. Han, W. Jiang, D. Niu, Y. Li, Y. Zhang, B. Lei, H. Liu, Y. Shi, B. Chen, L. Yin, X. Liu, D. Peng, B. Lu, *Adv. Intell. Syst.* **2019**, *1*, 1900109.
- [11] Y. Lee, W. J. Song, J. Y. Sun, *Mater. Today Phys.* **2020**, *15*, 100258.
- [12] M. Cianchetti, C. Laschi, A. Menciassi, P. Dario, *Nat. Rev. Mater.* **2018**, *3*, 143.
- [13] Z. Han, P. Wang, G. Mao, T. Yin, D. Zhong, B. Yiming, X. Hu, L. C. Jia, G. Nian, S. Qu, W. Yang, *ACS Appl. Mater. Interfaces* **2020**, *12*, 12010.
- [14] L. Wu, I. Chauhan, Y. Tadesse, *Adv. Mater. Technol.* **2018**, *3*, 1700359.
- [15] Z. Shen, F. Chen, X. Zhu, K.-T. Yong, G. Gu, *J. Mater. Chem. B* **2020**, *8*, 8972.
- [16] L. Ionov, *Mater. Today* **2014**, *17*, 494.
- [17] L. Ionov, *Adv. Funct. Mater.* **2013**, *23*, 4555.
- [18] J. Zheng, P. Xiao, X. Le, W. Lu, P. Théato, C. Ma, B. Du, J. Zhang, Y. Huang, T. Chen, *J. Mater. Chem. C* **2018**, *6*, 1320.
- [19] Q. Shi, H. Liu, D. Tang, Y. Li, X. Li, F. Xu, *NPG Asia Mater.* **2019**, *11*, 64.
- [20] E. Wang, M. S. Desai, S.-W. Lee, *Nano Lett.* **2013**, *13*, 2826.
- [21] C. Li, A. Iscen, H. Sai, K. Sato, N. A. Sather, S. M. Chin, Z. Álvarez, L. C. Palmer, G. C. Schatz, S. I. Stupp, *Nat. Mater.* **2020**, *19*, 900.
- [22] W. J. Zheng, N. An, J. H. Yang, J. Zhou, Y. M. Chen, *ACS Appl. Mater. Interfaces* **2015**, *7*, 1758.
- [23] L. Hua, M. Xie, Y. Jian, B. Wu, C. Chen, C. Zhao, *ACS Appl. Mater. Interfaces* **2019**, *11*, 43641.
- [24] H. Haider, C. H. Yang, W. J. Zheng, J. H. Yang, M. X. Wang, S. Yang, M. Zrínyi, Y. Osada, Z. Suo, Q. Zhang, J. Zhou, Y. M. Chen, *Soft Matter* **2015**, *11*, 8253.
- [25] S. Zhou, B. Wu, Q. Zhou, Y. Jian, X. Le, H. Lu, D. Zhang, J. Zhang, Z. Zhang, T. Chen, *Macromol. Rapid Commun.* **2020**, *41*, 1900543.
- [26] Q. Zhao, Y. Liang, L. Ren, Z. Yu, Z. Zhang, F. Qiu, L. Ren, *J. Mater. Chem. B* **2018**, *6*, 1260.

- [27] Y. Dong, J. Wang, X. Guo, S. Yang, M. O. Ozen, P. Chen, X. Liu, W. Du, F. Xiao, U. Demirci, B.-F. Liu, *Nat. Commun.* **2019**, *10*, 4087.
- [28] N. Bassik, B. T. Abebe, K. E. Laffin, D. H. Gracias, *Polymer* **2010**, *51*, 6093.
- [29] R. L. Truby, J. A. Lewis, *Nature* **2016**, *540*, 371.
- [30] J. Li, C. Wu, P. K. Chu, M. Gelinsky, *Mater. Sci. Eng., R* **2020**, *140*, 100543.
- [31] E. Sacyhani Keneth, A. Kamyshny, M. Totaro, L. Beccai, S. Magdassi, *Adv. Mater.* **2021**, *33*, 2003387.
- [32] H. Arslan, A. Nojoomi, J. Jeon, K. Yum, *Adv. Sci.* **2019**, *6*, 1800703.
- [33] A. Gevorkian, S. M. Morozova, S. Kheiri, N. Khuu, H. Chen, E. Young, N. Yan, E. Kumacheva, *Adv. Funct. Mater.* **2021**, *31*, 2010743.
- [34] J. Odent, S. Vanderstappen, A. Toncheva, E. Pichon, T. J. Wallin, K. Wang, R. F. Shepherd, P. Dubois, J.-M. Raquez, *J. Mater. Chem. A* **2019**, *7*, 15395.
- [35] D. Podstawczyk, M. Nizioł, P. Szymczyk-Ziółkowska, M. Fiedot-Toboła, *Adv. Funct. Mater.* **2021**, *31*, 2009664.
- [36] S. Y. Zheng, Y. Shen, F. Zhu, J. Yin, J. Qian, J. Fu, Z. L. Wu, Q. Zheng, *Adv. Funct. Mater.* **2018**, *28*, 1803366.
- [37] A. Sydney Gladman, E. A. Matsumoto, R. G. Nuzzo, L. Mahadevan, J. A. Lewis, *Nat. Mater.* **2016**, *15*, 413.
- [38] A. K. Mishra, W. Pan, E. P. Giannelis, R. F. Shepherd, T. J. Wallin, *Nat. Protoc.* **2021**, *16*, 2068.
- [39] F. M. Cheng, H. X. Chen, H.-d. Li, *J. Mater. Chem. B* **2021**, *9*, 1762.
- [40] J. M. McCracken, B. M. Rauzan, J. C. E. Kjellman, H. Su, S. A. Rogers, R. G. Nuzzo, *Adv. Funct. Mater.* **2019**, *29*, 1806723.
- [41] P. Wu, J. Wang, X. Wang, *Autom. Constr.* **2016**, *68*, 21.
- [42] L.-Y. Zhou, J. Fu, Y. He, *Adv. Funct. Mater.* **2020**, *30*, 2000187.
- [43] J. Z. Gul, M. Sajid, M. M. Rehman, G. U. Siddiqui, I. Shah, K.-H. Kim, J.-W. Lee, K. H. Choi, *Sci. Technol. Adv. Mater.* **2018**, *19*, 243.
- [44] F. Yang, V. Tadepalli, B. J. Wiley, *ACS Biomater. Sci. Eng.* **2017**, *3*, 863.
- [45] F. Zhu, L. Cheng, J. Yin, Z. L. Wu, J. Qian, J. Fu, Q. Zheng, *ACS Appl. Mater. Interfaces* **2016**, *8*, 31304.
- [46] S. V. Murphy, A. Atala, *Nat. Biotechnol.* **2014**, *32*, 773.
- [47] H. Li, C. Tan, L. Li, *Mater. Des.* **2018**, *159*, 20.
- [48] J. Z. Manapat, Q. Chen, P. Ye, R. C. Advincula, *Macromol. Mater. Eng.* **2017**, *302*, 1600553.
- [49] S. Derakhshanfar, R. Mbeleck, K. Xu, X. Zhang, W. Zhong, M. Xing, *Bioact. Mater.* **2018**, *3*, 144.
- [50] R. F. Pereira, P. J. Bártolo, *J. Appl. Polym. Sci.* **2015**, *132*, 42458.
- [51] J. K. Placone, A. J. Engler, *Adv. Healthcare Mater.* **2018**, *7*, 1701161.
- [52] S. Kyle, Z. M. Jessop, A. Al-Sabab, I. S. Whitaker, *Adv. Healthcare Mater.* **2017**, *6*, 1700264.
- [53] C. D. Armstrong, N. Todd, A. T. Alsharhan, D. I. Bigio, R. D. Sochol, *Adv. Mater. Technol.* **2021**, *6*, 2000829.
- [54] R. Michel, R. Auzély-Velty, *Biomacromolecules* **2020**, *21*, 2949.
- [55] C. Xu, G. Dai, Y. Hong, *Acta Biomater.* **2019**, *95*, 50.
- [56] C. W. Peak, J. Stein, K. A. Gold, A. K. Gaharwar, *Langmuir* **2018**, *34*, 917.
- [57] G. Cidonio, M. Glinka, J. I. Dawson, R. O. C. Oreffo, *Biomaterials* **2019**, *209*, 10.
- [58] K. Pataky, T. Braschler, A. Negro, P. Renaud, M. P. Lutolf, J. Brugger, *Adv. Mater.* **2012**, *24*, 391.
- [59] M. Guvendiren, J. Molde, R. M. D. Soares, J. Kohn, *ACS Biomater. Sci. Eng.* **2016**, *2*, 1679.
- [60] N. Hong, G.-H. Yang, J. Lee, G. Kim, *J. Biomed. Mater. Res., Part B* **2018**, *106*, 444.
- [61] F. Liu, C. Liu, Q. Chen, Q. Ao, X. Tian, J. Fan, H. Tong, X. Wang, *Int. J. Bioprint.* **2018**, *4*, 128.
- [62] M. Y. Teo, S. Kee, N. RaviChandran, L. Stuart, K. C. Aw, J. Stringer, *ACS Appl. Mater. Interfaces* **2020**, *12*, 1832.
- [63] K. Christensen, B. Davis, Y. Jin, Y. Huang, *Mater. Sci. Eng., C* **2018**, *89*, 65.
- [64] X. Peng, T. Liu, Q. Zhang, C. Shang, Q.-W. Bai, H. Wang, *Adv. Funct. Mater.* **2017**, *27*, 1701962.
- [65] X.-Q. Zhang, D. Wu, J.-B. Hou, J.-F. Feng, D. Ke, S. Zhang, B.-J. Li, *ACS Appl. Polym. Mater.* **2019**, *1*, 1187.
- [66] F. P. W. Melchels, J. Feijen, D. W. Grijpma, *Biomaterials* **2010**, *31*, 6121.
- [67] G. Burke, D. M. Devine, I. Major, *Polymers* **2020**, *12*, 2015.
- [68] H. Kumar, K. Sakthivel, M. G. A. Mohamed, E. Boras, S. R. Shin, K. Kim, *Macromol. Biosci.* **2021**, *21*, 2000317.
- [69] A. K. Mishra, T. J. Wallin, W. Pan, P. Xu, K. Wang, E. P. Giannelis, B. Mazzolai, R. F. Shepherd, *Sci. Rob.* **2020**, *5*, eaaz3918.
- [70] T. J. Wallin, J. H. Pikul, S. Bodkhe, B. N. Peele, B. C. Mac Murray, D. Therriault, B. W. McEnerney, R. P. Dillon, E. P. Giannelis, R. F. Shepherd, *J. Mater. Chem. B* **2017**, *5*, 6249.
- [71] A. A. Pawar, G. Saada, I. Cooperstein, L. Larush, J. A. Jackman, S. R. Tabaei, N.-J. Cho, S. Magdassi, *Sci. Adv.* **2016**, *2*, e1501381.
- [72] M. Layani, X. Wang, S. Magdassi, *Adv. Mater.* **2018**, *30*, 1706344.
- [73] Z. Ji, C. Yan, B. Yu, X. Zhang, M. Cai, X. Jia, X. Wang, F. Zhou, *Adv. Mater. Technol.* **2019**, *4*, 1800713.
- [74] D. Han, Z. Lu, S. A. Chester, H. Lee, *Sci. Rep.* **2018**, *8*, 1963.
- [75] V. Chan, J. H. Jeong, P. Bajaj, M. Collens, T. Saif, H. Kong, R. Bashir, *Lab Chip* **2012**, *12*, 88.
- [76] C. Sun, N. Fang, D. M. Wu, X. Zhang, *Sens. Actuators, A* **2005**, *121*, 113.
- [77] Q. Ge, Z. Li, Z. Wang, K. Kowsari, W. Zhang, X. He, J. Zhou, N. X. Fang, *Int. J. Extreme Manuf.* **2020**, *2*, 022004.
- [78] V. Harinarayana, Y. C. Shin, *Opt. Laser Technol.* **2021**, *142*, 107180.
- [79] J.-F. Xing, M. L. Zheng, X. M. Duan, *Chem. Soc. Rev.* **2015**, *44*, 5031.
- [80] D. M. Zuev, A. K. Nguyen, V. I. Putlyaev, R. J. Narayan, *Bioprinting* **2020**, *20*, e00090.
- [81] Z. Xiong, M. L. Zheng, X.-Z. Dong, W. Q. Chen, F. Jin, Z. S. Zhao, X. M. Duan, *Soft Matter* **2011**, *7*, 10353.
- [82] F. Gao, C. Ruan, W. Liu, *Mater. Chem. Front.* **2019**, *3*, 1736.
- [83] P. Heidarian, A. Z. Kouzani, A. Kaynak, M. Paulino, B. Nasri-Nasrabadi, *ACS Biomater. Sci. Eng.* **2019**, *5*, 2688.
- [84] Y. Jin, C. Liu, W. Chai, A. Compaan, Y. Huang, *ACS Appl. Mater. Interfaces* **2017**, *9*, 17456.
- [85] Z. Chen, D. Zhao, B. Liu, G. Nian, X. Li, J. Yin, S. Qu, W. Yang, *Adv. Funct. Mater.* **2019**, *29*, 1900971.
- [86] X. Xue, Y. Hu, Y. Deng, J. Su, *Adv. Funct. Mater.* **2021**, *31*, 2009432.
- [87] S. Uman, A. Dhand, J. A. Burdick, *J. Appl. Polym. Sci.* **2020**, *137*, 48668.
- [88] D. Zhao, Y. Liu, B. Liu, Z. Chen, G. Nian, S. Qu, W. Yang, *ACS Appl. Mater. Interfaces* **2021**, *13*, 13714.
- [89] F. L. C. Morgan, L. Moroni, M. B. Baker, *Adv. Healthcare Mater.* **2020**, *9*, 1901798.
- [90] T. Jungst, W. Smolan, K. Schacht, T. Scheibel, J. Groll, *Chem. Rev.* **2016**, *116*, 1496.
- [91] L. L. Wang, C. B. Highley, Y.-C. Yeh, J. H. Galarraga, S. Uman, J. A. Burdick, *J. Biomed. Mater. Res., Part A* **2018**, *106*, 865.
- [92] Z. Lei, Q. Wang, P. Wu, *Mater. Horiz.* **2017**, *4*, 694.
- [93] C. Loebel, C. B. Rodell, M. H. Chen, J. A. Burdick, *Nat. Protoc.* **2017**, *12*, 1521.
- [94] J. Gong, C. C. L. Schuurmans, A. M. v. Genderen, X. Cao, W. Li, F. Cheng, J. J. He, A. López, V. Huerta, J. Manríquez, R. Li, H. Li, C. Delavaux, S. Sebastian, P. E. Capendale, H. Wang, J. Xie, M. Yu, R. Masereeuw, T. Vermonden, Y. S. Zhang, *Nat. Commun.* **2020**, *11*, 1267.
- [95] J. Duan, X. Liang, K. Zhu, J. Guo, L. Zhang, *Soft Matter* **2017**, *13*, 345.
- [96] J. Li, Q. Ma, Y. Xu, M. Yang, Q. Wu, F. Wang, P. Sun, *ACS Appl. Mater. Interfaces* **2020**, *12*, 55290.

- [97] P. Sun, H. Zhang, D. Xu, Z. Wang, L. Wang, G. Gao, G. Hossain, J. Wu, R. Wang, J. Fu, *J. Mater. Chem. B* **2019**, *7*, 2619.
- [98] X. Liang, H. Ding, Q. Wang, M. Wang, B. Yin, G. Sun, *New J. Chem.* **2021**, *45*, 861.
- [99] Y. Hirokawa, T. Tanaka, *J. Chem. Phys.* **1984**, *81*, 6379.
- [100] L. Tavagnacco, E. Zaccarelli, E. Chiessi, *Phys. Chem. Chem. Phys.* **2018**, *20*, 9997.
- [101] J. Shang, P. Theato, *Soft Matter* **2018**, *14*, 8401.
- [102] J. R. Booth, R. A. Young, A. N. Richards Gonzales, Z. J. Meakin, C. M. Preuss-Weber, R. W. Jaggars, S. A. F. Bon, *J. Mater. Chem. C* **2021**, *9*, 7174.
- [103] C. d. I. H. Alarcón, S. Pennadam, C. Alexander, *Chem. Soc. Rev.* **2005**, *34*, 276.
- [104] J. Liu, W. Liu, A. Pantula, Z. Wang, D. H. Gracias, T. D. Nguyen, *Extreme Mech. Lett.* **2019**, *30*, 100514.
- [105] S. Naficy, R. Gately, R. GorkinIII, H. Xin, G. M. Spinks, *Macromol. Mater. Eng.* **2017**, *302*, 1600212.
- [106] T. Chen, H. Bakhshi, L. Liu, J. Ji, S. Agarwal, *Adv. Funct. Mater.* **2018**, *28*, 1800514.
- [107] M. C. Koetting, J. T. Peters, S. D. Steichen, N. A. Peppas, *Mater. Sci. Eng., R* **2015**, *93*, 1.
- [108] A. Augé, Y. Zhao, *RSC Adv.* **2016**, *6*, 70616.
- [109] Z. Xu, W. Liu, *Chem. Commun.* **2018**, *54*, 10540.
- [110] S. S. Athukorala, T. S. Tran, R. Balu, V. K. Truong, J. Chapman, N. K. Dutta, N. R. Choudhury, *Polymers* **2021**, *13*, 474.
- [111] S. Mondal, S. Das, A. K. Nandi, *Soft Matter* **2020**, *16*, 1404.
- [112] D. Han, C. Farino, C. Yang, T. Scott, D. Browe, W. Choi, J. W. Freeman, H. Lee, *ACS Appl. Mater. Interfaces* **2018**, *10*, 17512.
- [113] A. Zolfagharian, A. Z. Kouzani, S. Y. Khoo, B. Nasri-Nasrabadi, A. Kaynak, *Sens. Actuators, A* **2017**, *265*, 94.
- [114] A. Zolfagharian, A. Kaynak, S. Y. Khoo, A. Z. Kouzani, *3D Print. Addit. Manuf.* **2018**, *5*, 138.
- [115] A. López-Díaz, A. Martín-Pacheco, A. M. Rodríguez, M. A. Herrero, A. S. Vázquez, E. Vázquez, *Adv. Funct. Mater.* **2020**, *30*, 2004417.
- [116] Y. Li, G. Huang, X. Zhang, B. Li, Y. Chen, T. Lu, T. J. Lu, F. Xu, *Adv. Funct. Mater.* **2013**, *23*, 660.
- [117] M. V. Patton, P. Ryan, T. Calascione, N. Fischer, A. Morgenstern, N. Stenger, B. B. Nelson-Cheeseman, *Addit. Manuf.* **2019**, *27*, 482.
- [118] D. Podstawczyk, M. Nizioł, P. Szymczyk, P. Wiśniewski, A. Guiseppi-Elie, *Addit. Manuf.* **2020**, *34*, 101275.
- [119] H. Shinoda, S. Azukizawa, K. Maeda, F. Tsumori, *J. Electrochem. Soc.* **2019**, *166*, B3235.
- [120] R. Tognato, A. R. Armiento, V. Bonfrate, R. Levato, J. Malda, M. Alini, D. Eglin, G. Giancane, T. Serra, *Adv. Funct. Mater.* **2019**, *29*, 1804647.
- [121] C. Lv, H. Xia, Q. Shi, G. Wang, Y.-S. Wang, Q.-D. Chen, Y.-L. Zhang, L.-Q. Liu, H.-B. Sun, *Adv. Mater. Interfaces* **2017**, *4*, 1601002.
- [122] A. Le Duigou, G. Chabaud, F. Scarpa, M. Castro, *Adv. Funct. Mater.* **2019**, *29*, 1903280.
- [123] C. Lv, X.-C. Sun, H. Xia, Y.-H. Yu, G. Wang, X.-W. Cao, S.-X. Li, Y.-S. Wang, Q.-D. Chen, Y.-D. Yu, H.-B. Sun, *Sens. Actuators, B* **2018**, *259*, 736.



Fatih Puza worked at the Leibniz Institute for New Materials (INM, Saarbrücken, Germany) as a Ph.D. student and received his Ph.D. in chemistry from Saarland University (Saarbrücken, Germany) in 2021. He then joined the group of Prof. Dr. Karen Lienkamp as a postdoctoral researcher at the Freiburg Center for Interactive Materials and Bioinspired Technologies (FIT, Albert-Ludwigs-Universität, Freiburg, Germany), and later at the Materials Science Department at Saarland University. His current research focuses on 3D printable hydrogels and their soft actuator applications.



Karen Lienkamp studied Chemistry at the University of Cambridge and the Freie Universität. She worked at the Max Planck Institute for Polymer Research and received her Ph.D. in Chemistry from the Johannes Gutenberg-Universität (Mainz, Germany). After postdoctoral work at the Polymer Science and Engineering Department of the University of Massachusetts Amherst (Amherst, MA, USA), she headed a research group at the Albert-Ludwigs-Universität (Freiburg, Germany). Lienkamp's work was supported by numerous competitive grants, including the Emmy-Noether-Grant of the German Research Foundation (DFG), a Starting Grant of the European Research Council (ERC), and the Heisenberg Program of the DFG. Her current research focuses on bioinspired and biomimetic polymer materials.